Supporting Information

Copper Chloride Catalysis: Do μ_4-Oxido Copper Clusters Play a Significant Role?

Sabine Becker[†,§], Maximilian Dürr[±,§], Andreas Miska[†], Jonathan Becker[†], Christopher Gawlig[†], Ulrich Behrens[‡], Ivana Ivanović-Burmazović[±] and Siegfried Schindler[*,†]

[†]Justus-Liebig-Universität Gießen, Institut für Anorganische und Analytische Chemie, Heinrich-Buff-Ring 17, 35392 Gießen, Germany

[±]Friedrich-Alexander-Universität Erlangen-Nürnberg, Lehrstuhl für Bioanorganische Chemie, Egerlandstraße 1, 91058 Erlangen, Germany

‡Universität Hamburg, Institut für Anorganische und Angewandte Chemie, Martin-Luther-King-Platz 6, 20146 Hamburg, Germany

1. Materials and Methods

1.1 Chemicals and solvents

All chemicals used were of p.a. quality and were purchased from either Acros, Aldrich, Fluka or Merck, if not mentioned otherwise. Dry solvents for air sensitive reactions were redistilled under argon.

1.2 Air sensitive compounds

The preparation and handling of air sensitive compounds were performed under an argon atmosphere. For reactions and preparations either glove boxes from MBraun (equipped with water and dioxygen sensors) or standard Schlenk techniques were used.

1.3 Crystallography

Single crystals suitable for X-ray diffraction were mounted on the tip of a glass rod using inert perfluoropolyether oil. The X-ray crystallographic data were collected on a BRUKER NONIUS KappaCCD equipped with low temperature systems. In addition for data collection a BRUKER D8 Venture system equipped with dual IμS microfocus sources, a PHOTON100 detector and an OXFORD CRYOSYSTEMS 700 low temperature system was used. Data collection was performed using Mo-K_α radiation with wavelength 0.71073 Å and a collimating Quazar multilayer mirror. Semi-empirical absorption correction from equivalents was applied using SADABS-2014/4 and the structure was solved by intrinsic phasing using SHELXT2014.[1] The structures were solved by direct methods in SHELXS97 and SHELXL 2013 and refined by using full-matrix least squares in SHELXL97. Crystallographic data of the reported structures have been deposited with the Cambridge Crystallographic Data Centre as supplementary publication. For the corresponding numbers please see tables of crystal data and structure refinement for the specific compound. Copies of the data can be obtained, free of charge from the Cambridge Crystallographic Data Centre via www.ccdc.cam.ac.uk/data_request/cif. The crystallographic data for some compounds were not deposited because the crystals diffracted rather weakly or the structures are already known in literature.

1.4 Mass spectrometry

Cryospray-ionization MS (CSI-MS) measurements were performed on a UHR-TOF Bruker Daltonik (Bremen, Germany) maXis plus 5G, an ESI-ToF MS capable of resolution of at least 60,000FWHM, which was coupled to a Bruker Daltonik Cryospray unit. Detection was in both ion modes, the source voltage was 4.5 kV in positive ion mode and 2.6 kV in negative ion mode. The flow rates were 280 µL/hour. The drying gas (N_2), to aid solvent removal, was held at -35°C and the spray gas was held at -40°C. In source collision induced decomposition (isCID) was achieved by increasing the DC potential between funnel 1 and funnel 2 in the double stage ion funnel transfer zone which leads to decomposition of dimeric and oligomeric ion moieties formed during the ionization process. The ISCID energy was held at 25 eV for the concerning experiment. The machine was calibrated prior to every experiment via direct infusion of the Agilent ESI-TOF low concentration tuning mixture, which provided an m/z range of singly charged peaks up to 2700 Da in both ion modes.

1.5 Infrared spectroscopy and elemental analyses

All IR measurements were performed on Jasco FT/IR 4100. If not mentioned otherwise all samples were measured as KBr-pellet.

All measurements concerning elemental analysis were carried out using a Carlo-Erba 1106 CHN.

2. Crystallographic Data

3.1 Compound 1: $[CuCl_2(H_2O)]\cdot 0.5$ acetone

Table S1. Crystal data and structure refinement for compound **1**.

CCDC-no.	Not submitted.	
Diffractometer type	BRUKER Nonius FR591 with Kappa CCD	
Empirical formula	$C_{1.50}H_5Cl_2CuO_{1.50}$	
Formula weight	181.49	
Temperature	190(2) K	
Wavelength	0.71073 Å	
Crystal system	Monoclinic	
Space group	*C2/m*	
Unit cell dimensions	a = 17.836(4) Å	α= 90°.
	b = 3.2840(10) Å	β= 93.88(3)°.
	c = 9.593(2) Å	γ= 90°.
Volume	560.6(2) $Å^3$	
Z	4	
Density (calculated)	2.150 Mg/m^3	
Absorption coefficient	4.713 mm^{-1}	
F(000)	356	
Habitus, color	Needle, orange	
Crystal size	0.50 x 0.03 x 0.01 mm^3	
Theta range for data collection	2.128 to 24.976°.	
Index ranges	-20<=h<=19, -3<=k<=3, -11<=l<=11	
Reflections collected	1775	
Independent reflections	577 [R(int) = 0.0540]	
Completeness to theta = 24.976°	99.0 %	
Absorption correction	Semi-empirical from equivalents	
Refinement method	Full-matrix least-squares on F^2	
Data / restraints / parameters	577 / 4 / 52	
Goodness-of-fit on F^2	1.184	
Final R indices [I>2sigma(I)]	R1 = 0.0469, wR2 = 0.0987	
R indices (all data)	R1 = 0.0656, wR2 = 0.1101	
Extinction coefficient	n/a	
Largest diff. peak and hole	0.723 and -0.647 $e.Å^{-3}$	

The refinement shows half of the complex molecule in the independent unit of the elementary cell. All hydrogen atoms were found and isotropically refined. All non-hydrogen atoms were refined anisotropically, semi-empirical absorption corrections were applied.

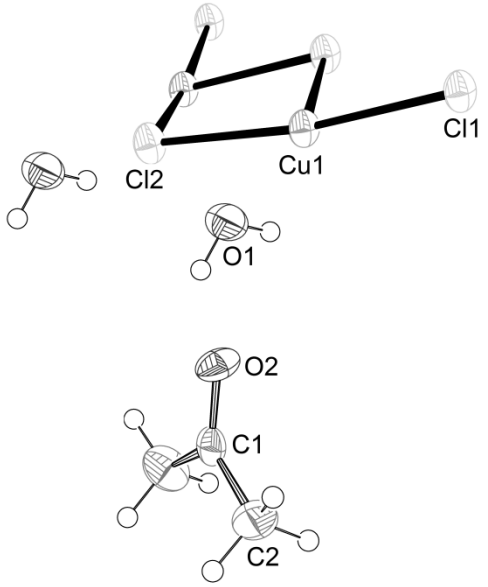

Figure S1: ORTEP plot with thermal ellipsoids set at 50% probability shows an excerpt of compound **1**.

Table S2. Selected bond lengths [Å] and angles [°] for compound **1**.

Cu(1)-Cl(2)#1	2.2761(18)
Cu(1)-Cl(2)	2.2761(18)
Cu(1)-Cl(1)	2.2825(18)
Cu(1)-Cl(1)#1	2.2825(18)
Cu(1)-O(1)	2.286(7)
Cl(1)-Cu(1)#2	2.2825(18)
Cl(2)-Cu(1)#2	2.2761(18)

Cl(2)#1-Cu(1)-Cl(2)	92.34(9)
Cl(2)#1-Cu(1)-Cl(1)	171.93(9)
Cl(2)-Cu(1)-Cl(1)	87.26(6)
Cl(2)#1-Cu(1)-Cl(1)#1	87.26(6)
Cl(2)-Cu(1)-Cl(1)#1	171.93(9)
Cl(1)-Cu(1)-Cl(1)#1	92.01(9)
Cl(2)#1-Cu(1)-O(1)	94.73(13)
Cl(2)-Cu(1)-O(1)	94.73(14)
Cl(1)-Cu(1)-O(1)	93.34(14)
Cl(1)#1-Cu(1)-O(1)	93.34(14)
Cu(1)#2-Cl(1)-Cu(1)	92.01(9)
Cu(1)#2-Cl(2)-Cu(1)	92.34(9)
Cu(1)-O(1)-H(1)	127(2)
Cu(1)-O(1)-H(2)	127(2)

Symmetry transformations used to generate equivalent atoms:

#1 x,y-1,z #2 x,y+1,z #3 x,-y+1,z

3.2 Compound 2: $[Cu_2(acetonitrile)_2Cl_4]$

Table S3. Crystal data and structure refinement for compound **2**.

CCDC-no.	Not submitted.	
Diffractometer type	BRUKER Nonius FR591 with Kappa CCD	
Empirical formula	$C_4 H_6 Cl_4 Cu_2 N_2$	
Formula weight	350.99	
Temperature	190(2) K	
Wavelength	0.71073 Å	
Crystal system	Monoclinic	
Space group	$P2_1/c$	
Unit cell dimensions	a = 3.7990(8) Å	α= 90°.
	b = 7.9080(16) Å	β= 89.94(3)°.
	c = 18.075(4) Å	γ = 90°.
Volume	543.02(19) $Å^3$	
Z	2	
Density (calculated)	2.147 Mg/m^3	
Absorption coefficient	4.847 mm^{-1}	
F(000)	340	
Crystal size	0.750 x 0.050 x 0.020 mm^3	
Theta range for data collection	2.576 to 27.574°.	
Index ranges	-4<=h<=4, -10<=k<=7, -22<=l<=23	
Reflections collected	3334	
Independent reflections	1213 [R(int) = 0.1491]	
Completeness to theta = 25.242°	99.5 %	
Absorption correction	Empirical	
Max. and min. transmission	0.49496 and 0.11067	
Refinement method	Full-matrix least-squares on F^2	
Data / restraints / parameters	1213 / 0 / 57	
Goodness-of-fit on F^2	1.041	
Final R indices [I>2sigma(I)]	R1 = 0.0747, wR2 = 0.1936	
R indices (all data)	R1 = 0.0959, wR2 = 0.2093	
Extinction coefficient	n/a	
Largest diff. peak and hole	1.877 and -1.361 e.$Å^{-3}$	

The structure was solved as twin (TWIN 1 0 0 0 -1 0 0 0 1, BASF 0.45521). The refinement shows half of the complex molecule in the independent unit of the elementary cell. All hydrogen atoms were positioned geometrically and isotropically refined. All non-hydrogen atoms were refined anisotropically, semiempirical absorption corrections were applied.

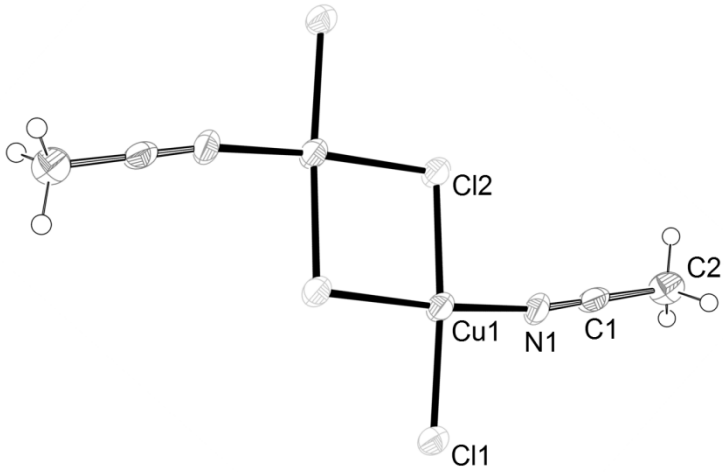

Figure S2: ORTEP plot with thermal ellipsoids set at 50% probability shows the full compound **2**.

T*able S4*. Selected bond lengths [Å] and angles [°] for compound **2**.

Cu(1)-N(1)	1.967(8)
Cu(1)-Cl(2)	2.236(3)
Cu(1)-Cl(1)	2.293(3)
Cu(1)-Cl(1)#1	2.310(3)
Cl(1)-Cu(1)#1	2.310(3)
N(1)-Cu(1)-Cl(2)	93.1(3)
N(1)-Cu(1)-Cl(1)	172.6(3)
Cl(2)-Cu(1)-Cl(1)	92.48(10)
N(1)-Cu(1)-Cl(1)#1	88.3(3)
Cl(2)-Cu(1)-Cl(1)#1	172.89(14)
Cl(1)-Cu(1)-Cl(1)#1	85.59(10)
Cu(1)-Cl(1)-Cu(1)#1	94.41(10)
C(1)-N(1)-Cu(1)	168.0(11)

Symmetry transformations used to generate equivalent atoms:
#1 -x+1,-y+1,-z+1

3.3 Compound 3: [Cu_3(acetonitrile)$_2Cl_6$]

Table S5. Crystal data and structure refinement for compound **3**.

CCDC-no.	982980	
Diffractometer type	BRUKER Nonius FR591 with Kappa CCD	
Empirical formula	C_4 H_6 Cl_6 Cu_3 N_2	
Formula weight	485.43	
Temperature	190(2) K	
Wavelength	0.71073 Å	
Crystal system	Monoclinic	
Space group	$P2_1/c$	
Unit cell dimensions	a = 6.737(2) Å	α= 90°.
	b = 6.1293(15) Å	β= 105.91(3)°.
	c = 16.438(6) Å	γ = 90°.

Volume	652.8(4) $Å^3$
Z	2
Density (calculated)	2.470 Mg/m^3
Absorption coefficient	6.035 mm^{-1}
F(000)	466
Crystal size	0.400 x 0.400 x 0.200 mm^3
Theta range for data collection	3.144 to 25.022°.
Index ranges	-8<=h<=8, -7<=k<=7, -19<=l<=19
Reflections collected	9662
Independent reflections	1152 [R(int) = 0.0490]
Completeness to theta = 25.022°	99.9 %
Absorption correction	Semi-empirical from equivalents
Max. and min. transmission	0.7456 and 0.4216
Refinement method	Full-matrix least-squares on F^2
Data / restraints / parameters	1152 / 0 / 72
Goodness-of-fit on F^2	1.134
Final R indices [I>2sigma(I)]	R1 = 0.0209, wR2 = 0.0459
R indices (all data)	R1 = 0.0236, wR2 = 0.0467
Extinction coefficient	0.0035(6)
Largest diff. peak and hole	0.315 and -0.337 $e.Å^{-3}$

The refinement shows half the molecule in the independent unit of the elementary cell. All hydrogen atoms were positioned geometrically and isotropically refined. All non-hydrogen atoms were refined anisotropically. Semi-empirical absorption corrections were applied.

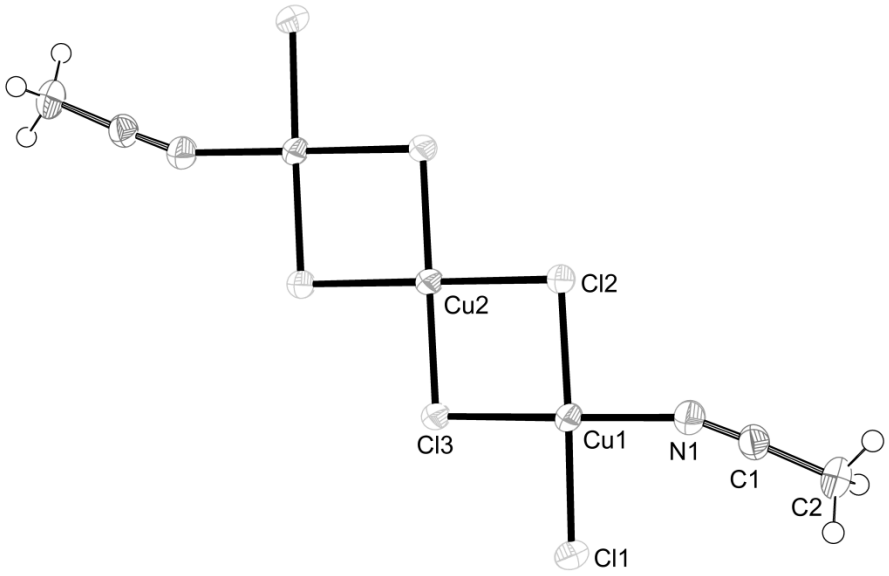

Figure S3: ORTEP plot with thermal ellipsoids set at 50% probability shows the full compound **3**.

Table S6. Selected bond lengths [Å] and angles [°] for compound **3**.

Cu(1)-N(1)	1.986(2)
Cu(1)-Cl(1)	2.2624(8)
Cu(1)-Cl(3)	2.3003(9)
Cu(1)-Cl(2)	2.3014(8)
Cu(1)-Cl(1)#1	2.6984(10)

Cu(2)-Cl(3)#2	2.2667(8)
Cu(2)-Cl(3)	2.2667(8)
Cu(2)-Cl(2)	2.2833(9)
Cu(2)-Cl(2)#2	2.2833(9)
Cl(1)-Cu(1)#1	2.6984(10)

N(1)-Cu(1)-Cl(1)	89.09(7)
N(1)-Cu(1)-Cl(3)	170.81(7)
Cl(1)-Cu(1)-Cl(3)	91.11(3)
N(1)-Cu(1)-Cl(2)	93.40(7)
Cl(1)-Cu(1)-Cl(2)	173.73(3)
Cl(3)-Cu(1)-Cl(2)	85.51(3)
N(1)-Cu(1)-Cl(1)#1	89.02(7)
Cl(1)-Cu(1)-Cl(1)#1	92.13(3)
Cl(3)-Cu(1)-Cl(1)#1	100.15(3)
Cl(2)-Cu(1)-Cl(1)#1	93.67(3)
Cl(3)#2-Cu(2)-Cl(3)	180.0
Cl(3)#2-Cu(2)-Cl(2)	93.28(3)
Cl(3)-Cu(2)-Cl(2)	86.72(3)
Cl(3)#2-Cu(2)-Cl(2)#2	86.72(3)
Cl(3)-Cu(2)-Cl(2)#2	93.28(3)
Cl(2)-Cu(2)-Cl(2)#2	180.00(3)
Cu(1)-Cl(1)-Cu(1)#1	87.87(3)
Cu(2)-Cl(2)-Cu(1)	93.64(3)
Cu(2)-Cl(3)-Cu(1)	94.11(3)
C(1)-N(1)-Cu(1)	159.0(2)

Symmetry transformations used to generate equivalent atoms:
#1 -x+2,-y+1,-z+1 #2 -x+1,-y+2,-z+1

3.4 Compound 4: $[Cu_3Cl_6(THF)_4]$

Table S7. Crystal data and structure refinement for compound **4**.

CCDC-no.	Not submitted.	
Diffractometer type	BRUKER D8 Venture	
Empirical formula	$C_{16}\ H_{32}\ Cl_6\ Cu_3\ O_4$	
Formula weight	691.73	
Temperature	100(2) K	
Wavelength	0.71073 Å	
Crystal system	Monoclinic	
Space group	*Cm*	
Unit cell dimensions	a = 11.376(2) Å	α= 90°.
	b = 11.0267(19) Å	β= 91.499(10)°.
	c = 9.7439(18) Å	γ = 90°.
Volume	1221.8(4) $Å^3$	
Z	2	
Density (calculated)	1.880 Mg/m^3	
Absorption coefficient	3.264 mm^{-1}	
F(000)	698	
Crystal size	2.458 x 0.182 x 0.101 mm^3	
Theta range for data collection	3.583 to 24.970°.	
Index ranges	-13<=h<=13, -13<=k<=13, -11<=l<=11	

Reflections collected	9655
Independent reflections	2237 [R(int) = 0.0701]
Completeness to theta = 24.970°	99.5 %
Absorption correction	Semi-empirical from equivalents
Max. and min. transmission	0.7452 and 0.3511
Refinement method	Full-matrix least-squares on F^2
Data / restraints / parameters	2237 / 229 / 171
Goodness-of-fit on F^2	1.133
Final R indices [I>2sigma(I)]	R1 = 0.0794, wR2 = 0.1764
R indices (all data)	R1 = 0.1012, wR2 = 0.1943
Extinction coefficient	n/a
Largest diff. peak and hole	1.916 and -1.810 e.$Å^{-3}$

The refinement shows half of the complex molecule in the independent unit of the elementary cell. All hydrogen atoms were positioned geometrically. All non-hydrogen atoms were refined anisotropically, semi-empirical absorption corrections were applied.

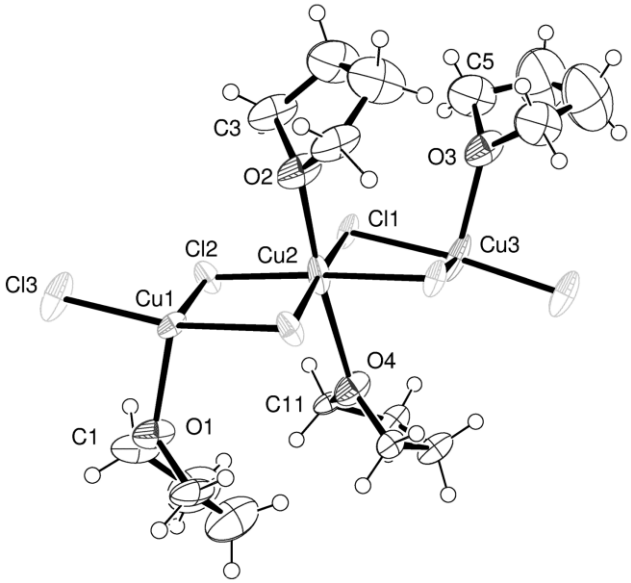

Figure S4: ORTEP plot with thermal ellipsoids set at 50% probability shows an excerpt of compound **4**.

Table S8. Selected bond lengths [Å] and angles [°] for compound **4**.

Cu(1)-O(1)	2.19(2)
Cu(1)-Cl(2)	2.293(8)
Cu(1)-Cl(2)#1	2.293(8)
Cu(1)-Cl(3)	2.293(9)
Cu(1)-Cl(3)#1	2.293(9)
Cu(2)-O(2)	2.25(3)
Cu(2)-Cl(2)#1	2.267(8)
Cu(2)-Cl(2)	2.267(8)
Cu(2)-Cl(1)	2.291(8)
Cu(2)-Cl(1)#1	2.291(8)
Cu(2)-O(4)	2.71(5)
Cu(3)-Cl(3)#2	2.286(8)
Cu(3)-Cl(3)#3	2.286(8)
Cu(3)-Cl(1)#1	2.288(8)

Cu(3)-Cl(1)	2.288(8)
Cu(3)-O(3)	2.29(4)
Cu(3)-O(5)	2.53(6)
Cl(3)-Cu(3)#4	2.286(8)

O(1)-Cu(1)-Cl(2)	101.4(8)
O(1)-Cu(1)-Cl(2)#1	101.4(8)
Cl(2)-Cu(1)-Cl(2)#1	87.3(4)
O(1)-Cu(1)-Cl(3)	91.1(9)
Cl(2)-Cu(1)-Cl(3)	91.6(2)
Cl(2)#1-Cu(1)-Cl(3)	167.5(3)
O(1)-Cu(1)-Cl(3)#1	91.1(9)
Cl(2)-Cu(1)-Cl(3)#1	167.5(3)
Cl(2)#1-Cu(1)-Cl(3)#1	91.6(2)
Cl(3)-Cu(1)-Cl(3)#1	86.9(4)
O(2)-Cu(2)-Cl(2)#1	88.1(7)
O(2)-Cu(2)-Cl(2)	88.1(7)
Cl(2)#1-Cu(2)-Cl(2)	88.5(4)
O(2)-Cu(2)-Cl(1)	95.6(7)
Cl(2)#1-Cu(2)-Cl(1)	176.3(4)
Cl(2)-Cu(2)-Cl(1)	92.2(2)
O(2)-Cu(2)-Cl(1)#1	95.6(7)
Cl(2)#1-Cu(2)-Cl(1)#1	92.2(2)
Cl(2)-Cu(2)-Cl(1)#1	176.3(4)
Cl(1)-Cu(2)-Cl(1)#1	86.9(4)
O(2)-Cu(2)-O(4)	174.5(18)
Cl(2)#1-Cu(2)-O(4)	95.9(10)
Cl(2)-Cu(2)-O(4)	95.9(10)
Cl(1)-Cu(2)-O(4)	80.4(10)
Cl(1)#1-Cu(2)-O(4)	80.4(10)
Cl(3)#2-Cu(3)-Cl(3)#3	87.2(4)
Cl(3)#2-Cu(3)-Cl(1)#1	92.6(2)
Cl(3)#3-Cu(3)-Cl(1)#1	174.8(5)
Cl(3)#2-Cu(3)-Cl(1)	174.8(5)
Cl(3)#3-Cu(3)-Cl(1)	92.6(2)
Cl(1)#1-Cu(3)-Cl(1)	87.1(4)
Cl(3)#2-Cu(3)-O(3)	93.5(8)
Cl(3)#3-Cu(3)-O(3)	93.5(8)
Cl(1)#1-Cu(3)-O(3)	91.6(7)
Cl(1)-Cu(3)-O(3)	91.6(7)
Cl(3)#2-Cu(3)-O(5)	89.7(10)
Cl(3)#3-Cu(3)-O(5)	89.7(10)
Cl(1)#1-Cu(3)-O(5)	85.2(10)
Cl(1)-Cu(3)-O(5)	85.2(10)
O(3)-Cu(3)-O(5)	175.5(18)
Cu(3)-Cl(1)-Cu(2)	91.7(2)
Cu(2)-Cl(2)-Cu(1)	92.0(3)
Cu(3)#4-Cl(3)-Cu(1)	92.7(3)
C(1)-O(1)-C(1)#1	108.2(18)
C(1)-O(1)-Cu(1)	122.3(12)
C(1)#1-O(1)-Cu(1)	122.3(12)

Symmetry transformations used to generate equivalent atoms:
#1 x,-y+1,z #2 x,-y+1,z-1 #3 x,y,z-1 #4 x,y,z+1

3.5 Compound 5: $[Cu(DMSO)_2Cl_2]$

Table S9. Crystal data and structure refinement for compound **5**.

CCDC-no.	Not submitted	
Diffractometer type	BRUKER Nonius FR591 with Kappa CCD	
Empirical formula	$C_4 H_{12} Cl_2 Cu O_2 S_2$	
Formula weight	290.70	
Temperature	190(2) K	
Wavelength	0.71073 Å	
Crystal system	Orthorhombic	
Space group	*Pnma*	
Unit cell dimensions	a = 7.9620(16) Å	α= 90°.
	b = 11.483(2) Å	β= 90°.
	c = 11.325(2) Å	γ = 90°.
Volume	1035.4(4) $Å^3$	
Z	4	
Density (calculated)	1.865 Mg/m^3	
Absorption coefficient	2.982 mm^{-1}	
F(000)	588	
Crystal size	0.700 x 0.300 x 0.080 mm^3	
Theta range for data collection	2.526 to 27.516°.	
Index ranges	-8<=h<=10, -12<=k<=14, -12<=l<=14	
Reflections collected	4534	
Independent reflections	1247 [R(int) = 0.0315]	
Completeness to theta = 25.242°	100.0 %	
Absorption correction	Semi-empirical from equivalents	
Max. and min. transmission	0.7456 and 0.4680	
Refinement method	Full-matrix least-squares on F^2	
Data / restraints / parameters	1247 / 0 / 58	
Goodness-of-fit on F^2	1.066	
Final R indices [I>2sigma(I)]	R1 = 0.0229, wR2 = 0.0566	
R indices (all data)	R1 = 0.0288, wR2 = 0.0588	
Extinction coefficient	0.0073(8)	
Largest diff. peak and hole	0.414 and -0.459 $e.Å^{-3}$	

The refinement shows half the molecule in the independent unit of the elementary cell. All hydrogen atoms were positioned geometrically and isotropically refined. All non-hydrogen atoms were refined anisotropically, semi-empirical absorption corrections were applied.

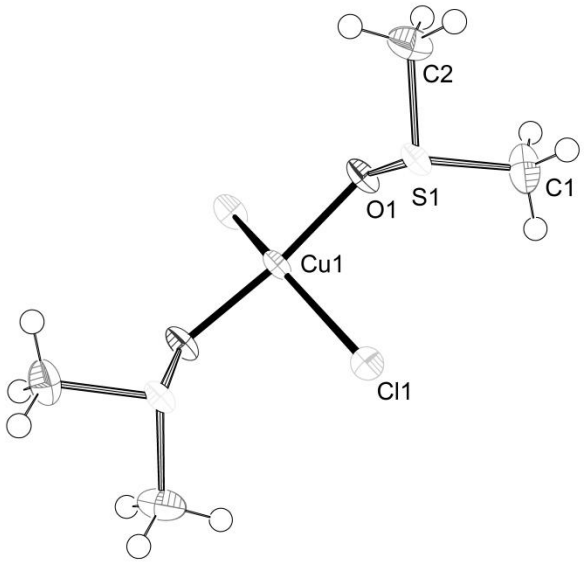

Figure S5: ORTEP plot with thermal ellipsoids set at 50% probability shows the full compound **5**.

Table S10. Selected bond lengths [Å] and angles [°] for compound **5**.

Cu(1)-O(1)#1	1.9498(14)
Cu(1)-O(1)	1.9498(14)
Cu(1)-Cl(1)	2.2806(9)
Cu(1)-Cl(2)	2.2871(7)
Cu(1)-Cl(2)#2	2.6660(8)
Cl(2)-Cu(1)#3	2.6660(8)

O(1)#1-Cu(1)-O(1)	173.62(8)
O(1)#1-Cu(1)-Cl(1)	92.73(4)
O(1)-Cu(1)-Cl(1)	92.73(4)
O(1)#1-Cu(1)-Cl(2)	88.65(4)
O(1)-Cu(1)-Cl(2)	88.65(4)
Cl(1)-Cu(1)-Cl(2)	146.25(3)
O(1)#1-Cu(1)-Cl(2)#2	87.85(4)
O(1)-Cu(1)-Cl(2)#2	87.85(4)
Cl(1)-Cu(1)-Cl(2)#2	101.29(3)
Cl(2)-Cu(1)-Cl(2)#2	112.46(2)
S(1)-O(1)-Cu(1)	117.63(7)
Cu(1)-Cl(2)-Cu(1)#3	144.00(3)

Symmetry transformations used to generate equivalent atoms:
#1 x,-y+3/2,z #2 x+1/2,y,-z+1/2 #3 x-1/2,y,-z+1/2

3.6 Compound 6: $(H_2N(CH_3)_2)_2[CuCl_3]$

Table S11. Crystal data and structure refinement for compound **6**.

CCDC-no.	982981
Diffractometer type	BRUKER Nonius FR591 with Kappa CCD
Empirical formula	$C_4\ H_{16}\ Cl_3\ Cu\ N_2$
Formula weight	262.08

Temperature	190(2) K	
Wavelength	0.71073 Å	
Crystal system	Triclinic	
Space group	$P\bar{1}$	
Unit cell dimensions	a = 7.2930(15) Å	α= 113.14(3)°.
	b = 9.0060(18) Å	β= 100.38(3)°.
	c = 9.6850(19) Å	γ = 100.33(3)°.
Volume	553.0(2) $Å^3$	
Z	2	
Density (calculated)	1.574 Mg/m^3	
Absorption coefficient	2.644 mm^{-1}	
F(000)	268	
Crystal size	0.700 x 0.450 x 0.250 mm^3	
Theta range for data collection	2.380 to 26.370°.	
Index ranges	-9<=h<=9, -10<=k<=11, -12<=l<=12	
Reflections collected	7665	
Independent reflections	2257 [R(int) = 0.0270]	
Completeness to theta = 25.242°	99.9 %	
Absorption correction	Semi-empirical from equivalents	
Max. and min. transmission	0.7456 and 0.5016	
Refinement method	Full-matrix least-squares on F^2	
Data / restraints / parameters	2257 / 0 / 155	
Goodness-of-fit on F^2	1.051	
Final R indices [I>2sigma(I)]	R1 = 0.0253, wR2 = 0.0588	
R indices (all data)	R1 = 0.0305, wR2 = 0.0607	
Largest diff. peak and hole	0.256 and -0.775 $e.Å^{-3}$	

The refinement shows one molecule in the independent unit of the elementary cell. All hydrogen atoms were found and isotropically refined. All non-hydrogen atoms were refined anisotropically. Semi-empirical absorption corrections were applied.

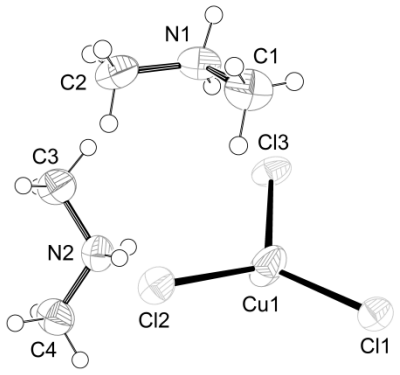

Figure S6: ORTEP plot with thermal ellipsoids set at 50% probability shows the full compound
6.

T*able S12*. Selected bond lengths [Å] and angles [°] for compound **6**.

C(1)-N(1)	1.474(3)
C(2)-N(1)	1.472(3)

C(3)-N(2)	1.471(3)
C(4)-N(2)	1.477(3)
Cl(1)-Cu(1)	2.2719(10)
Cl(2)-Cu(1)	2.2814(12)
Cl(3)-Cu(1)	2.2667(7)

Cl(3)-Cu(1)-Cl(1)	115.39(4)
Cl(3)-Cu(1)-Cl(2)	117.39(3)
Cl(1)-Cu(1)-Cl(2)	122.04(4)
C(2)-N(1)-C(1)	114.3(2)
C(3)-N(2)-C(4)	112.8(2)

3.7 Compound 8: $[Cu_4OCl_6(CH_3CN)_4]\cdot 2CH_3CN$

Table S13. Crystal data and structure refinement for compound **8**.

Diffractometer type	BRUKER D8 Venture	
Empirical formula	$C_{12}H_{18}Cl_6Cu_4N_6O$	
Formula weight	729.18	
Temperature	100(2) K	
Wavelength	0.71073 Å	
Crystal system	Monoclinic	
Space group	*C*2/*c*	
Unit cell dimensions	a = 8.7364(8) Å	a= 90°.
	b = 24.201(2) Å	b= 94.709(3)°.
	c = 12.3458(10) Å	g = 90°.
Volume	2601.4(4) $Å^3$	
Z	4	
Density (calculated)	1.862 Mg/m^3	
Absorption coefficient	3.857 mm^{-1}	
F(000)	1432	
Habitus, color	Plate, red	
Crystal size	0.266 x 0.186 x 0.078 mm^3	
Theta range for data collection	2.879 to 43.240°.	
Index ranges	-16<=h<=16, -46<=k<=46, -23<=l<=23	
Reflections collected	75815	
Independent reflections	9723 [R(int) = 0.0585]	
Completeness to theta = 25.242°	99.7 %	
Absorption correction	Semi-empirical from equivalents	
Max. and min. transmission	0.7485 and 0.5976	
Refinement method	Full-matrix least-squares on F^2	
Data / restraints / parameters	9723 / 0 / 136	
Goodness-of-fit on F^2	1.126	
Final R indices [I>2sigma(I)]	R1 = 0.0488, wR2 = 0.0771	
R indices (all data)	R1 = 0.0705, wR2 = 0.0824	
Largest diff. peak and hole	1.028 and -0.948 $e.Å^{-3}$	

The refinement shows one molecule in the independent unit of the elementary cell. All hydrogen atoms were calculated and isotropically refined. All non-hydrogen atoms were refined anisotropically. Absorption corrections were applied.

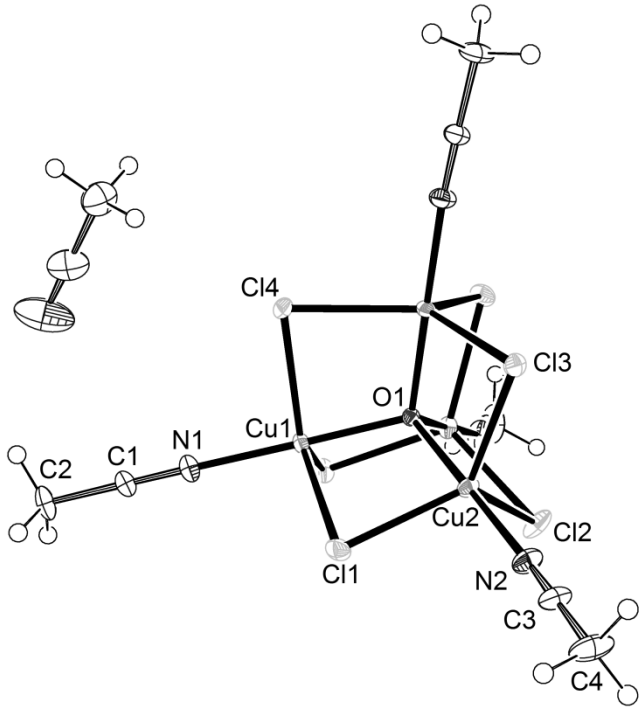

Figure S7: ORTEP plot with thermal ellipsoids set at 50% probability shows the full compound **8**. For clarity only one free acetonitrile solvent molecule is shown.

T*able S14*. Selected bond lengths [Å] and angles [°] for compound **8**.

Cu(1)-O(1)	1.9020(8)
Cu(1)-N(1)	1.9319(13)
Cu(1)-Cl(3)#1	2.3811(4)
Cu(1)-Cl(4)	2.3856(4)
Cu(1)-Cl(1)	2.4006(4)
C(1)-N(1)	1.1382(19)
C(1)-C(2)	1.447(2)
Cl(1)-Cu(2)	2.3848(4)
O(1)-Cu(2)#1	1.8999(8)
O(1)-Cu(2)	1.8999(8)
O(1)-Cu(1)#1	1.9021(8)
Cu(2)-N(2)	1.9574(14)
Cu(2)-Cl(3)	2.3600(4)
Cu(2)-Cl(2)	2.4365(4)
N(2)-C(3)	1.141(2)
Cl(2)-Cu(2)#1	2.4365(5)
Cl(3)-Cu(1)#1	2.3812(4)
C(3)-C(4)	1.449(2)
Cl(4)-Cu(1)#1	2.3856(4)
O(1)-Cu(1)-N(1)	177.47(5)
O(1)-Cu(1)-Cl(3)#1	84.29(2)
N(1)-Cu(1)-Cl(3)#1	93.46(4)
O(1)-Cu(1)-Cl(4)	84.27(3)
N(1)-Cu(1)-Cl(4)	95.97(4)
Cl(3)#1-Cu(1)-Cl(4)	121.627(12)

O(1)-Cu(1)-Cl(1)	84.96(2)
N(1)-Cu(1)-Cl(1)	97.07(5)
Cl(3)#1-Cu(1)-Cl(1)	115.484(16)
Cl(4)-Cu(1)-Cl(1)	120.161(13)
N(1)-C(1)-C(2)	178.51(18)
C(1)-N(1)-Cu(1)	172.80(14)
Cu(2)-Cl(1)-Cu(1)	80.582(13)
Cu(2)#1-O(1)-Cu(2)	110.78(7)
Cu(2)#1-O(1)-Cu(1)	109.084(9)
Cu(2)-O(1)-Cu(1)	108.971(9)
Cu(2)#1-O(1)-Cu(1)#1	108.971(9)
Cu(2)-O(1)-Cu(1)#1	109.087(9)
Cu(1)-O(1)-Cu(1)#1	109.94(7)
O(1)-Cu(2)-N(2)	177.22(6)
O(1)-Cu(2)-Cl(3)	84.925(19)
N(2)-Cu(2)-Cl(3)	93.49(5)
O(1)-Cu(2)-Cl(1)	85.45(2)
N(2)-Cu(2)-Cl(1)	93.57(5)
Cl(3)-Cu(2)-Cl(1)	124.073(16)
O(1)-Cu(2)-Cl(2)	84.69(4)
N(2)-Cu(2)-Cl(2)	98.07(5)
Cl(3)-Cu(2)-Cl(2)	115.937(13)
Cl(1)-Cu(2)-Cl(2)	117.757(13)
C(3)-N(2)-Cu(2)	166.88(15)
Cu(2)#1-Cl(2)-Cu(2)	79.847(18)
Cu(2)-Cl(3)-Cu(1)#1	81.563(13)
N(2)-C(3)-C(4)	179.7(2)
Cu(1)#1-Cl(4)-Cu(1)	81.518(17)

3.8 Compound 9: $[Cu_4OCl_6(THF)((NH_2)_2CO)_3]\cdot 3THF\cdot(NH_2)_2CO$

Table S15. Crystal data and structure refinement for compound **9**.

CCDC-no.	1417288	
Diffractometer type	BRUKER Nonius FR591 with Kappa CCD	
Empirical formula	$C_{20}H_{48}Cl_6Cu_4N_8O_9$	
Formula weight	1011.52	
Temperature	150(2) K	
Wavelength	0.71073 Å	
Crystal system	Triclinic	
Space group	$P\bar{1}$	
Unit cell dimensions	a = 9.924(2) Å	a= 84.35(3)°.
	b = 13.194(3) Å	b= 74.98(3)°.
	c = 15.652(3) Å	g = 74.68(3)°.
Volume	1908.1(8) $Å^3$	
Z	2	
Density (calculated)	1.761 Mg/m^3	
Absorption coefficient	2.673 mm^{-1}	
F(000)	1028	
Habitus, color	Block, yellow-green	
Crystal size	0.30 x 0.17 x 0.05 mm^3	
Theta range for data collection	2.373 to 25.026°.	
Index ranges	-11<=h<=11, -15<=k<=15, -18<=l<=18	

Reflections collected	43156
Independent reflections	6726 [R(int) = 0.1176]
Completeness to theta = 27.48°	99.9 %
Absorption correction	Empirical
Refinement method	Full-matrix least-squares on F^2
Data / restraints / parameters	6726 / 0 / 424
Goodness-of-fit on F^2	0.964
Final R indices [I>2sigma(I)]	R1 = 0.0332, wR2 = 0.0734
R indices (all data)	R1 = 0.0564, wR2 = 0.0796
Largest diff. peak and hole	0.890 and -0.528 e.$Å^{-3}$

The refinement shows one molecule in the independent unit of the elementary cell. All hydrogen atoms were calculated and isotropically refined. All non-hydrogen atoms were refined anisotropically. Absorption corrections were applied.

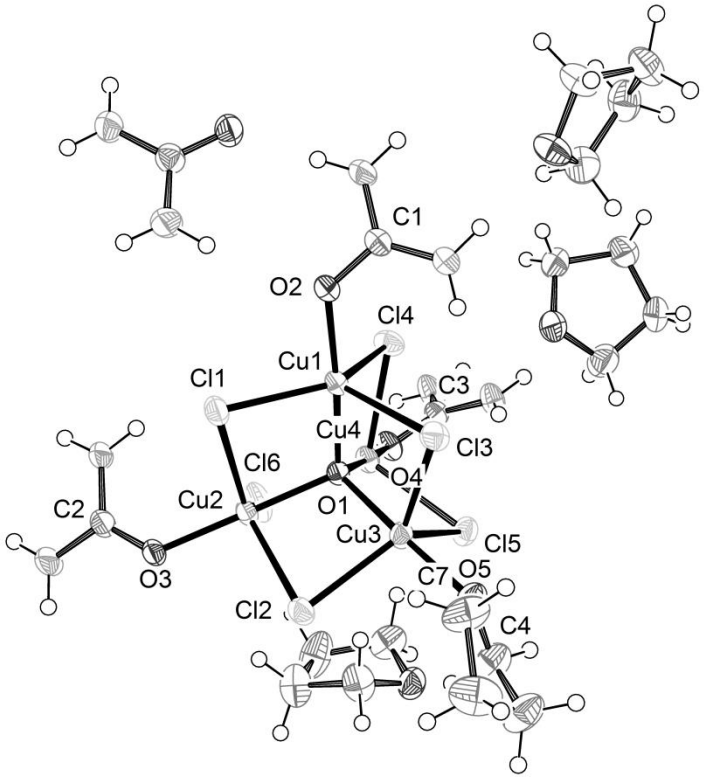

Figure S8: ORTEP plot with thermal ellipsoids set at 50% probability shows the full compound **9**.

T*able S16*. Selected bond lengths [Å] and angles [°] for compound **9**.

Cu(1)-O(1)	1.900(2)
Cu(1)-O(2)	1.912(2)
Cu(1)-Cl(1)	2.3538(12)
Cu(1)-Cl(4)	2.3622(12)
Cu(1)-Cl(3)	2.4871(13)
O(1)-Cu(2)	1.885(2)
O(1)-Cu(3)	1.891(2)
O(1)-Cu(4)	1.907(2)
Cu(2)-O(3)	1.915(2)
Cu(2)-Cl(6)	2.3681(13)

Cu(2)-Cl(2)	2.4175(12)
Cu(2)-Cl(1)	2.4297(11)
Cu(3)-O(5)	1.942(3)
Cu(3)-Cl(2)	2.3607(14)
Cu(3)-Cl(3)	2.3642(11)
Cu(3)-Cl(5)	2.4364(12)
Cu(4)-O(4)	1.933(2)
Cu(4)-Cl(6)	2.3649(14)
Cu(4)-Cl(4)	2.3880(12)
Cu(4)-Cl(5)	2.4240(12)
O(1)-Cu(1)-O(2)	174.84(11)
O(1)-Cu(1)-Cl(1)	85.48(7)
O(2)-Cu(1)-Cl(1)	91.05(7)
O(1)-Cu(1)-Cl(4)	85.29(7)
O(2)-Cu(1)-Cl(4)	94.33(8)
Cl(1)-Cu(1)-Cl(4)	132.92(5)
O(1)-Cu(1)-Cl(3)	83.51(8)
O(2)-Cu(1)-Cl(3)	101.49(9)
Cl(1)-Cu(1)-Cl(3)	117.12(4)
Cl(4)-Cu(1)-Cl(3)	107.48(4)
Cu(2)-O(1)-Cu(3)	108.99(11)
Cu(2)-O(1)-Cu(1)	109.71(10)
Cu(3)-O(1)-Cu(1)	109.64(12)
Cu(2)-O(1)-Cu(4)	109.95(12)
Cu(3)-O(1)-Cu(4)	110.03(10)
Cu(1)-O(1)-Cu(4)	108.51(11)
O(1)-Cu(2)-O(3)	178.58(11)
O(1)-Cu(2)-Cl(6)	84.19(8)
O(3)-Cu(2)-Cl(6)	94.42(9)
O(1)-Cu(2)-Cl(2)	84.73(8)
O(3)-Cu(2)-Cl(2)	96.25(8)
Cl(6)-Cu(2)-Cl(2)	121.57(4)
O(1)-Cu(2)-Cl(1)	83.66(7)
O(3)-Cu(2)-Cl(1)	96.87(8)
Cl(6)-Cu(2)-Cl(1)	122.47(5)
Cl(2)-Cu(2)-Cl(1)	112.91(5)
C(1)-O(2)-Cu(1)	125.4(2)
O(1)-Cu(3)-O(5)	177.92(10)
O(1)-Cu(3)-Cl(2)	86.22(7)
O(5)-Cu(3)-Cl(2)	95.86(8)
O(1)-Cu(3)-Cl(3)	87.19(8)
O(5)-Cu(3)-Cl(3)	91.77(9)
Cl(2)-Cu(3)-Cl(3)	124.96(4)
O(1)-Cu(3)-Cl(5)	85.13(7)
O(5)-Cu(3)-Cl(5)	93.56(8)
Cl(2)-Cu(3)-Cl(5)	122.72(4)
Cl(3)-Cu(3)-Cl(5)	111.00(4)
O(1)-Cu(4)-O(4)	176.04(10)
O(1)-Cu(4)-Cl(6)	83.81(8)
O(4)-Cu(4)-Cl(6)	92.60(8)
O(1)-Cu(4)-Cl(4)	84.41(7)
O(4)-Cu(4)-Cl(4)	96.26(8)
Cl(6)-Cu(4)-Cl(4)	123.89(4)
O(1)-Cu(4)-Cl(5)	85.14(8)
O(4)-Cu(4)-Cl(5)	98.28(8)
Cl(6)-Cu(4)-Cl(5)	123.84(4)

Cl(4)-Cu(4)-Cl(5)	109.44(5)
C(2)-O(3)-Cu(2)	125.0(2)
Cu(4)-Cl(5)-Cu(3)	79.60(4)
Cu(1)-Cl(1)-Cu(2)	80.60(4)
C(4)-O(5)-Cu(3)	120.0(3)
C(7)-O(5)-Cu(3)	118.2(2)
Cu(3)-Cl(2)-Cu(2)	80.06(4)
Cu(3)-Cl(3)-Cu(1)	79.33(4)
Cu(1)-Cl(4)-Cu(4)	81.13(4)
Cu(4)-Cl(6)-Cu(2)	81.99(5)
C(3)-O(4)-Cu(4)	127.9(2)

3. Mass spectrometry

4.1 $CuCl_2 \cdot 2H_2O$ in selected solvents

Methanol

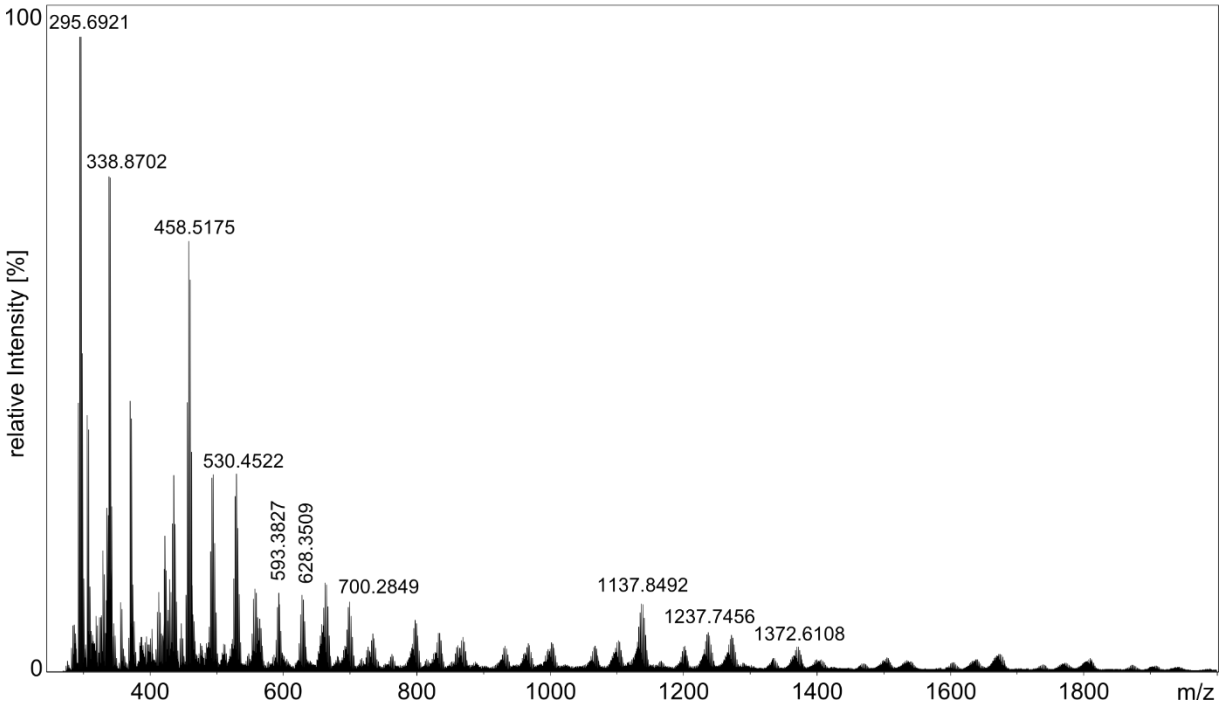

Figure S9: Mass spectrum of $CuCl_2 \cdot 2H_2O$ in methanol (50 mM, positive ion mode), the species identified are listed below. The oxidation states of the copper ions are mixed-valent.

Table S17: Observed species and m/z for $CuCl_2 \cdot 2H_2O$ in methanol (positive ion mode).

Species	**m/z**	**m/z calcd.**
$[Cu_3Cl_3]^+$	295.6921	295.6925
$[Cu_5Cl_4]^+$	458.5175	458.5184
$[Cu_5Cl_5]^+$	495.4835	495.4848
$[Cu_5Cl_6]$	530.4522	530.4535
$[Cu_6Cl_5]^+$	558.4188	558.4145
$[Cu_6Cl_6]^+$	593.3827	593.3832
$[Cu_6Cl_7]^+$	628.3509	628.3520
$[Cu_6Cl_9]^+$	700.2849	700.2870

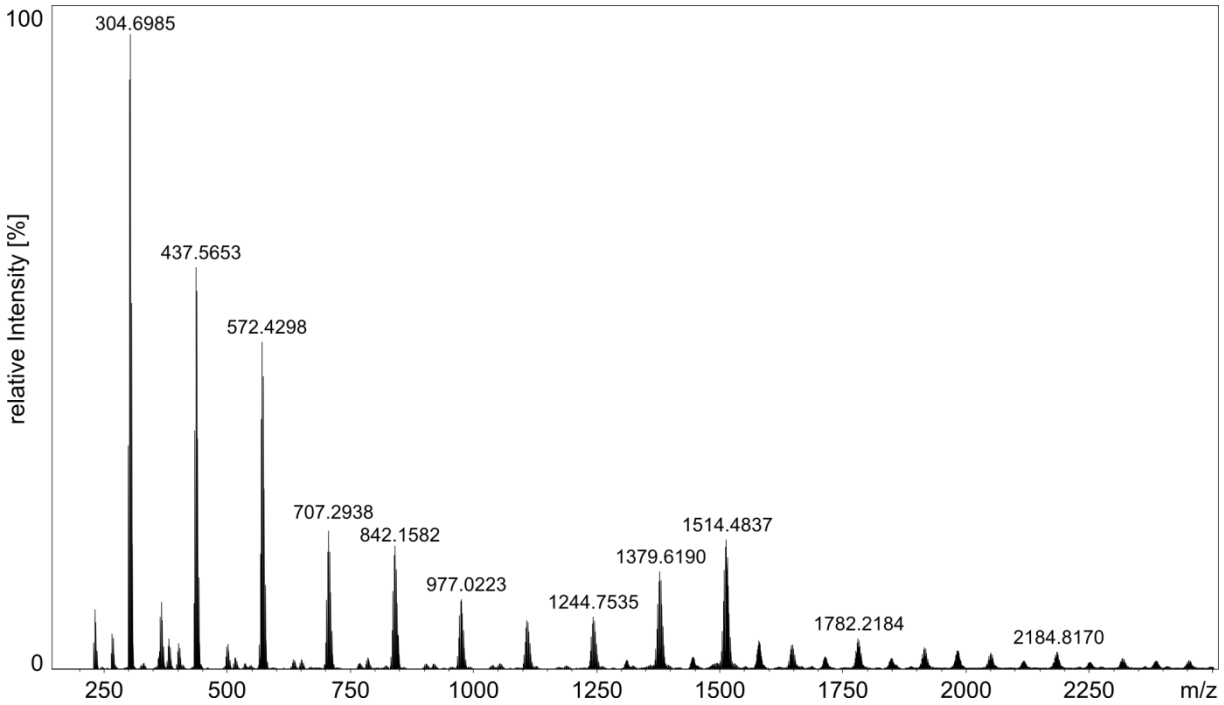

Figure 10: Mass spectrum of $CuCl_2 \cdot 2H_2O$ in methanol (50 mM, negative ion mode).

Table S18: Observed species and m/z for $CuCl_2 \cdot 2H_2O$ in methanol (negative ion mode).

Species	**m/z**	**m/z calcd.**
$[Cu_2Cl_5]^-$	304.6985	304.6989
$[Cu_3Cl_7]^-$	473.5653	473.5662
$[Cu_4Cl_9]^-$	572.4298	572.4310
$[Cu_5Cl_{11}]^-$	707.2938	707.2958
$[Cu_6Cl_{13}]^-$	842.1582	842.1606
$[Cu_7Cl_{15}]^-$	977.0223	977.0254
$[Cu_8Cl_{17}]^-$	1109.8889	1109.8927

Acetone

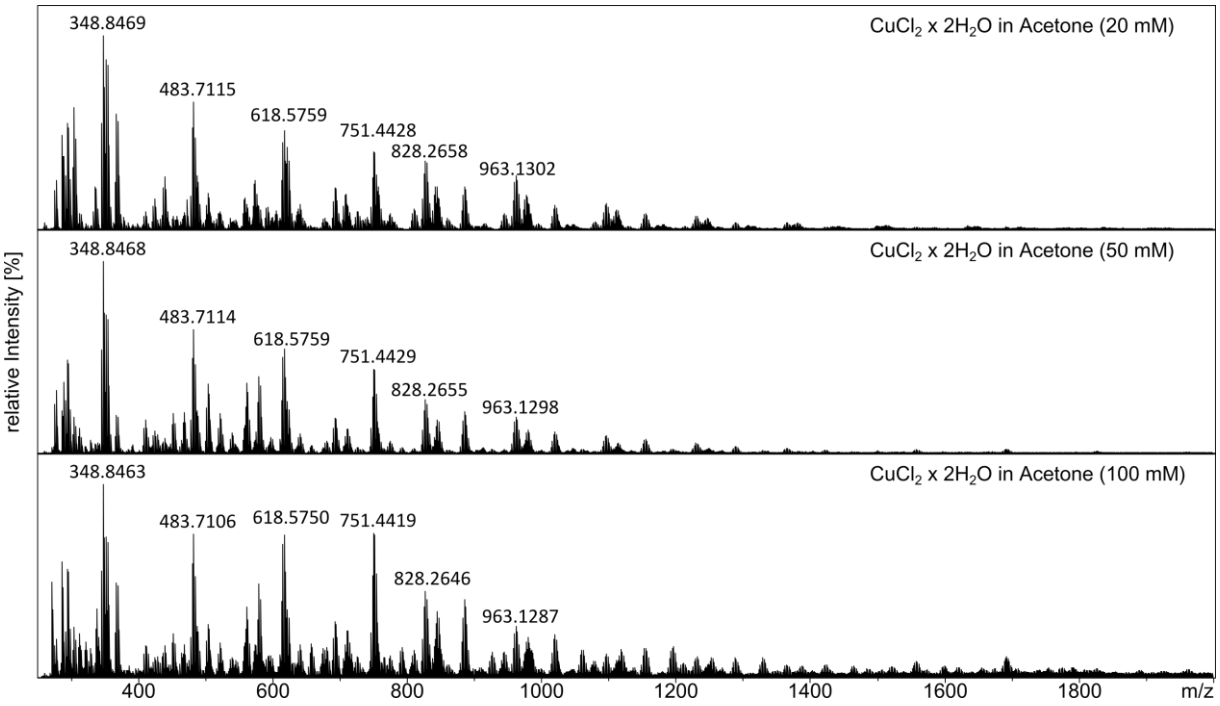

Figure S11: Mass spectrum of $CuCl_2 \cdot 2H_2O$ in acetone (positive ion mode), the species identified are listed below.

Table S19: Observed species and m/z for $CuCl_2 \cdot 2H_2O$ in acetone (positive ion mode).

Species	**m/z**	**m/z calcd.**
$[Cu_2Cl_3(C_3H_6O)_2]^+$	348.8469	348.8466
$[Cu_3Cl_5(C_3H_6O)_2]^+$	483.7121	483.7114
$[Cu_4Cl_7(C_3H_6O)_2]^+$	618.5759	618.5762
$[Cu_5Cl_9(C_3H_6O)_2]^+$	751.4434	751.4435
$[Cu_6Cl_{11}(C_3H_6O)]^+$	828.2658	828.2664
$[Cu_7Cl_{13}(C_3H_6O)]^+$	963.1302	963.1312
$[Cu_7Cl_{13}(C_3H_6O)_2]^+$	1021.1739	1012.1731

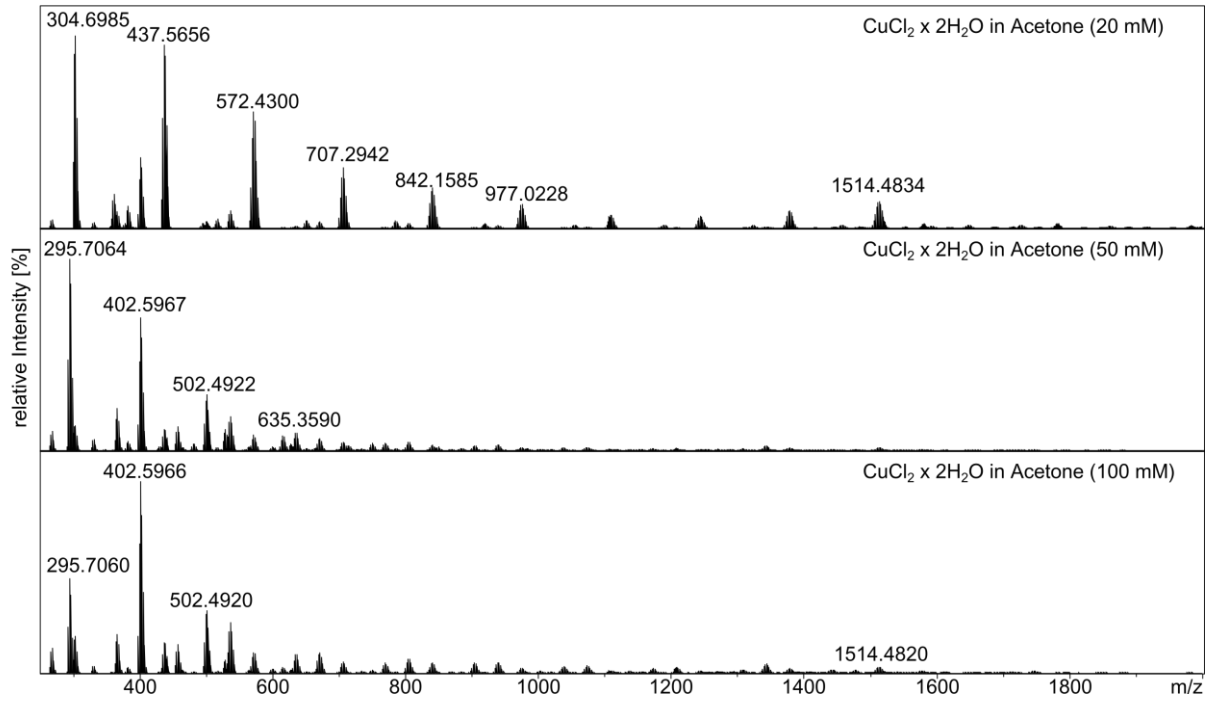

Figure S12: Mass spectrum of $CuCl_2 \cdot 2H_2O$ in acetone (negative ion mode), the species identified are listed below.

Table S20: Observed species and m/z for $CuCl_2 \cdot 2H_2O$ in acetone (negative ion mode).

Species	**m/z**	**m/z calcd.**
$[Cu_3Cl_5]^-$	367.6282	367.6277
$[Cu_3Cl_6]^-$	402.5975	402.5967
$[Cu_3Cl_7]^-$	437.5662	437.5648
$[Cu_4Cl_7]^-$	502.4935	502.4922
$[Cu_4Cl_8]^-$	537.4623	537.4607
$[Cu_4Cl_9]^-$	572.4310	572.4291
$[Cu_5Cl_{11}]^-$	707.2942	707.2958
$[Cu_6Cl_{13}]^-$	842.1585	842.1606

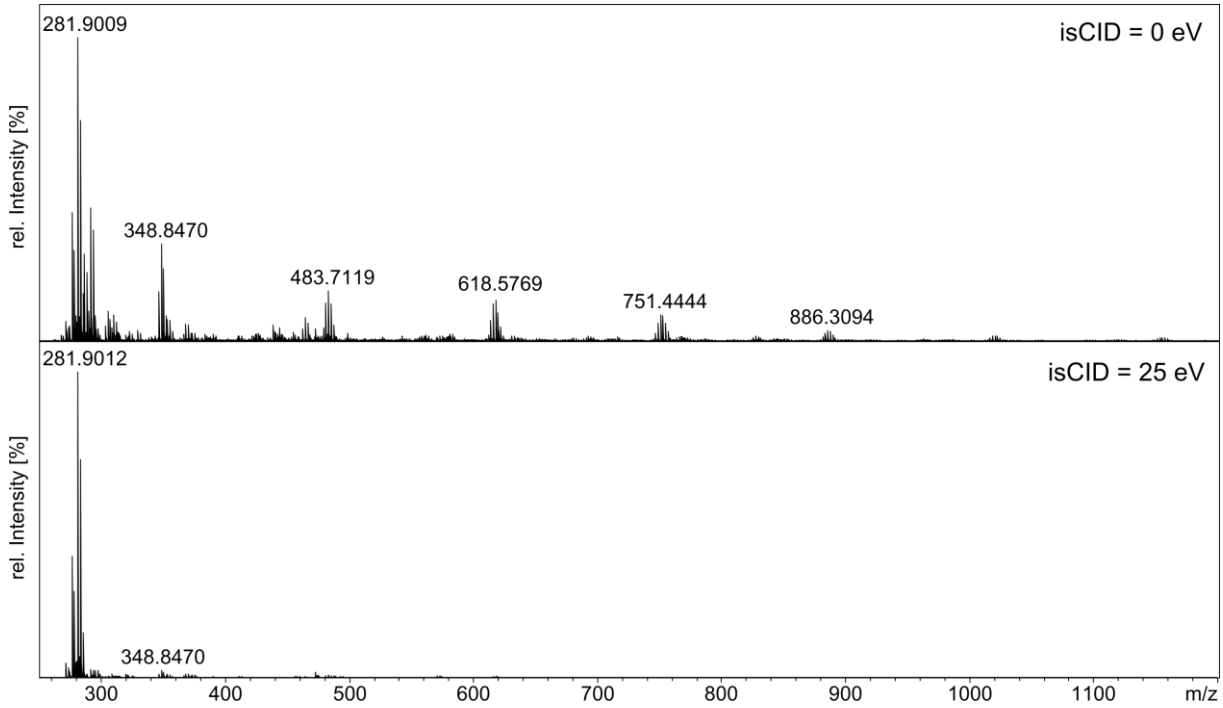

Figure S13: Comparison of mass spectrum of 50 mM $CuCl_2 \cdot 2H_2O$ in acetone with and without isCID, showing the disappearance of oligomeric structures upon using isCID.

Acetonitrile

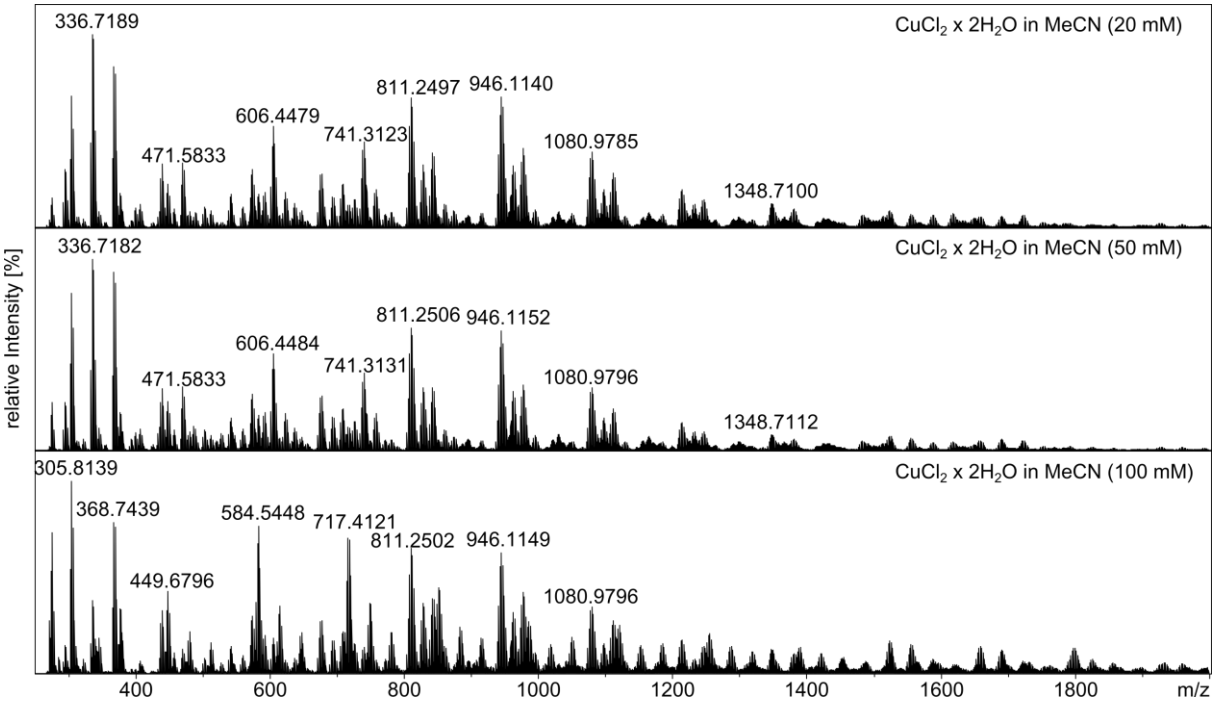

Figure S14: Mass spectrum of $CuCl_2 \cdot 2H_2O$ in acetonitrile (positive ion mode).

Table S21: Observed species and m/z for $CuCl_2 \cdot 2H_2O$ in acetonitrile (positive ion mode).

Species	**m/z**	**m/z calcd.**
$[Cu_3Cl_3(CH_3CN)]^+$	336.7189	336.7191
$[Cu_4Cl_5(CH_3CN)]^+$	471.5833	471.5839
$[Cu_5Cl_7(CH_3CN)]^+$	606.4479	606.4488
$[Cu_5Cl_9(CH_3CN)]^+$	678.3826	678.3838
$[Cu_6Cl_9(CH_3CN)]^+$	741.3123	741.3136
$[Cu_6Cl_{11}(CH_3CN)]^+$	811.2497	811.2511
$[Cu_6Cl_{11}(CH_3CN)(H_2O)]^+$	829.2600	829.2616
$[Cu_7Cl_{13}(CH_3CN)]^+$	946.1140	946.1159
$[Cu_7Cl_{13}(CH_3CN)(H_2O)]^+$	964.1245	964.1246

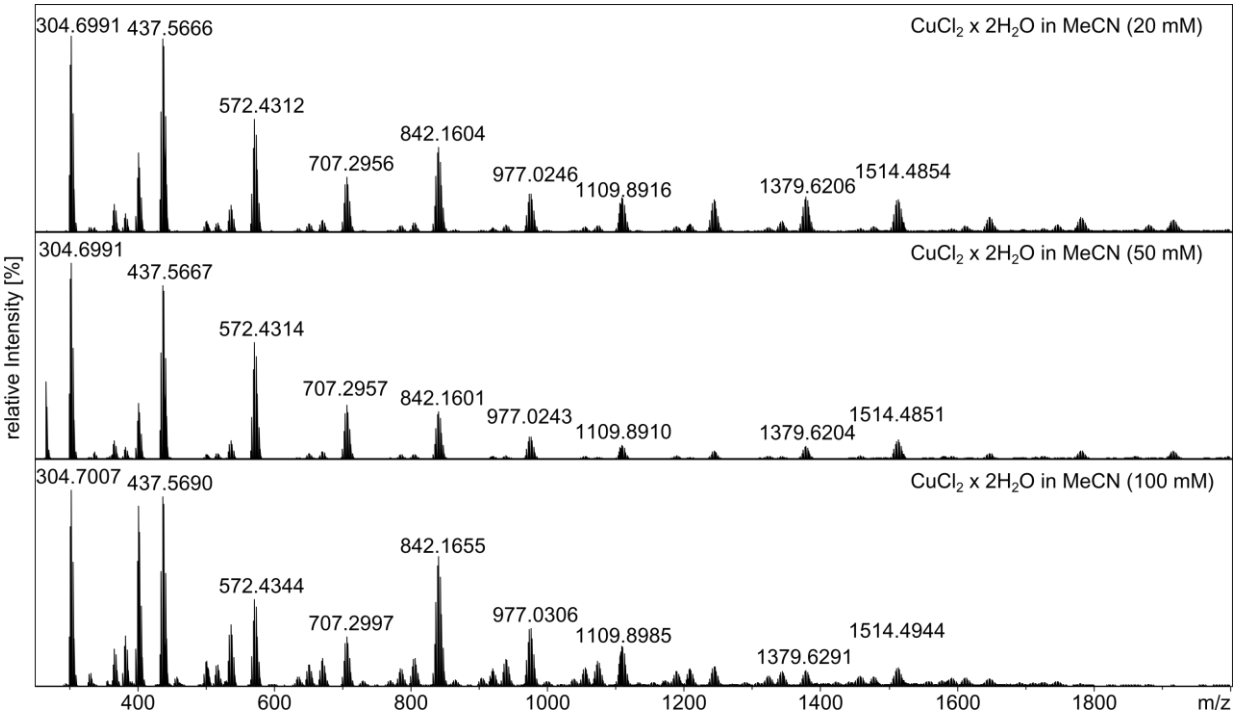

Figure S15: Mass spectrum of $CuCl_2 \cdot 2H_2O$ in acetonitrile (negative ion mode).

Table S22: Observed species and m/z for $CuCl_2 \cdot 2H_2O$ in acetonitrile (negative ion mode).

Species	**m/z**	**m/z calcd.**
$[Cu_2Cl_5]^-$	304.6991	304.6989
$[Cu_3Cl_7]^-$	437.5666	437.5662
$[Cu_4Cl_9]^-$	572.4312	572.4310
$[Cu_5Cl_{11}]^-$	707.2956	707.2958
$[Cu_6Cl_{13}]^-$	842.1604	842.1606
$[Cu_7Cl_{15}]^-$	977.0246	977.0254

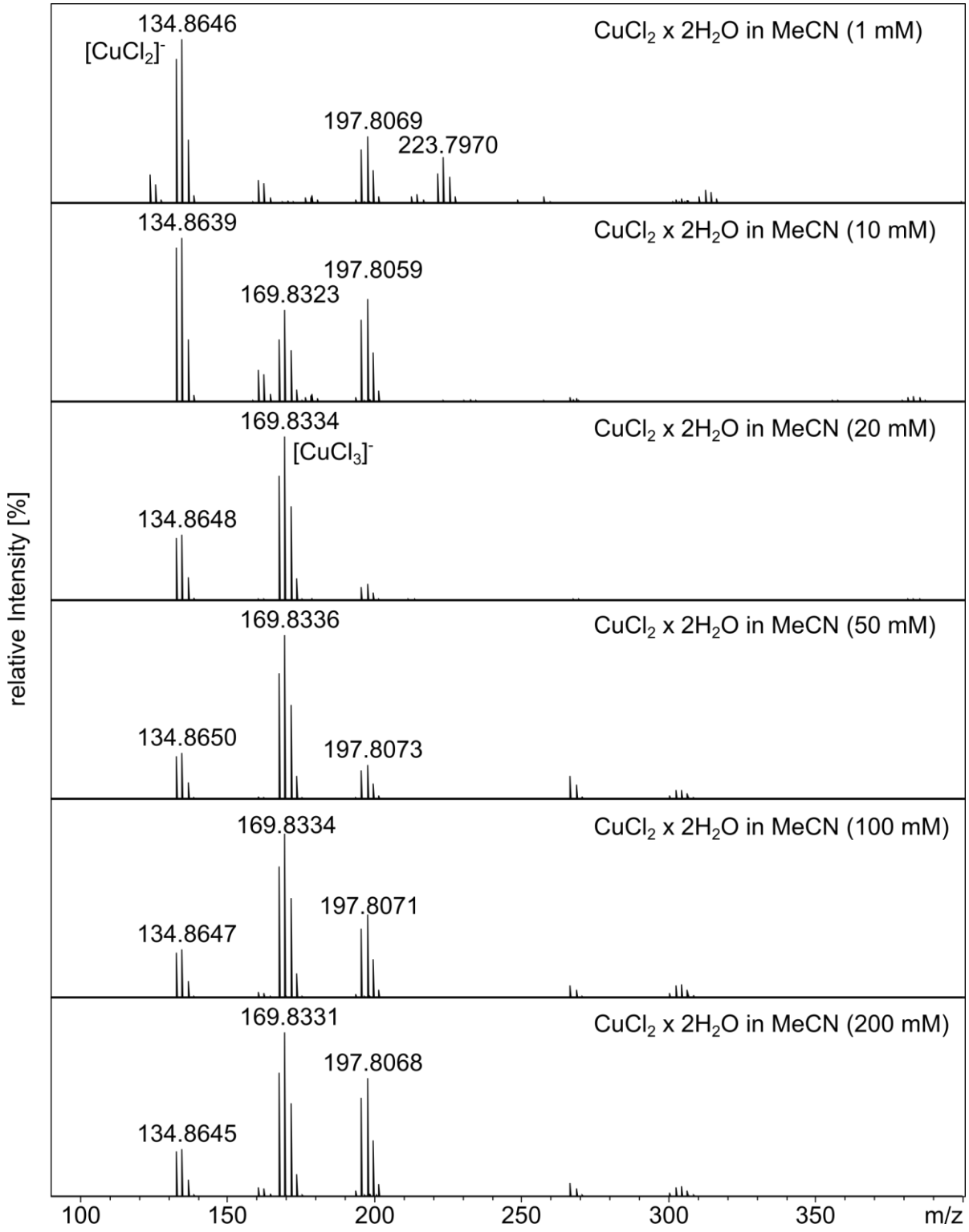

Figure S16: Mass spectrum of $CuCl_2 \cdot 2H_2O$ in acetonitrile (negative ion mode, different concentrations). This shows the concentration-dependence of the relative quantities of $[CuCl_2]^-$ (134.8650 m/z) to $[CuCl_3]^-$ (169.8336 m/z) and therefore the relative quantities of Cu(I) to Cu(II).

THF

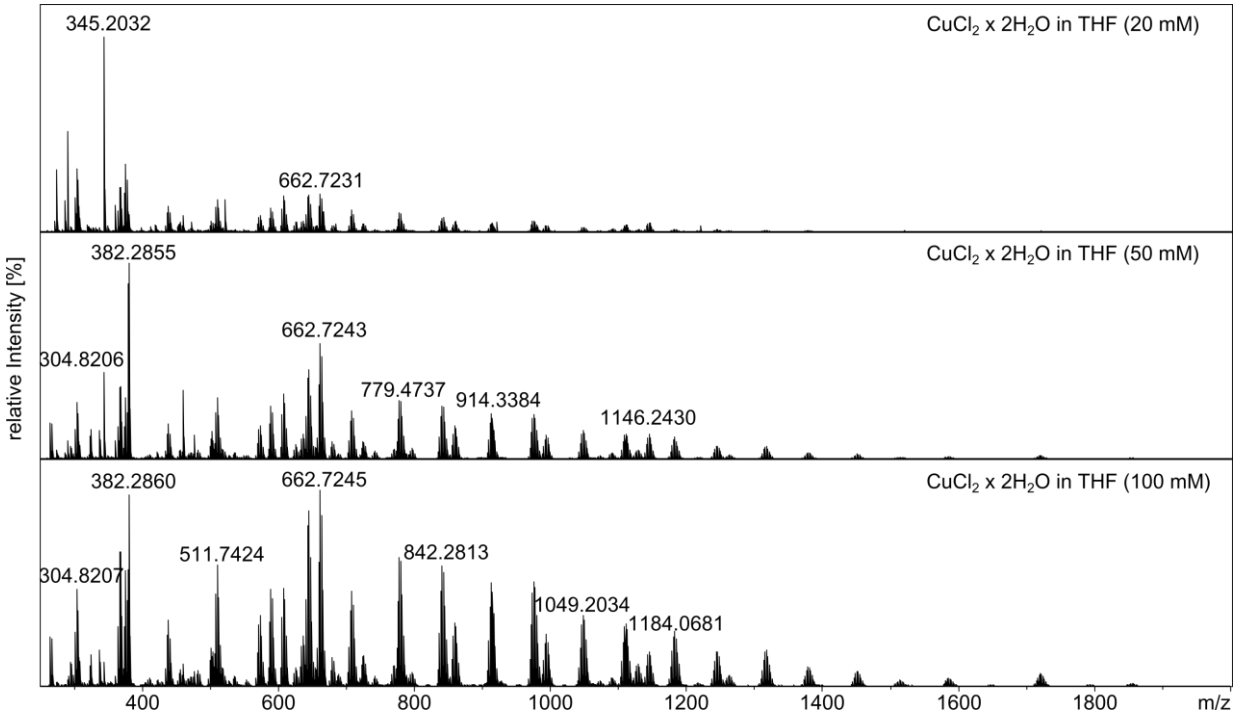

Figure S17: Mass spectrum of $CuCl_2 \cdot 2H_2O$ in THF (positive ion mode), the species identified are listed below.

Table S23: Observed species and m/z for $CuCl_2 \cdot 2H_2O$ in THF (positive ion mode).

Species	**m/z**	**m/z calcd.**
$[Cu_2Cl_3(C_4H_8O)]^+$	304.8200	304.8203
$[Cu_3Cl_5(C_4H_8O)]^+$	439.6849	439.6851
$[Cu_3Cl_5(C_4H_8O)_2]^+$	511.7424	511.7427
$[Cu_4Cl_7(C_4H_8O)]^+$	574.5494	574.5499
$[Cu_4Cl_7(C_4H_8O)_2]^+$	646.6072	646.6075
$[Cu_5Cl_9(C_4H_8O)_2]^+$	779.4740	779.4748
$[Cu_6Cl_{11}(C_4H_8O)]^+$	842.2830	842.2820
$[Cu_7Cl_{13}(C_4H_8O)]^+$	977.1465	977.1468

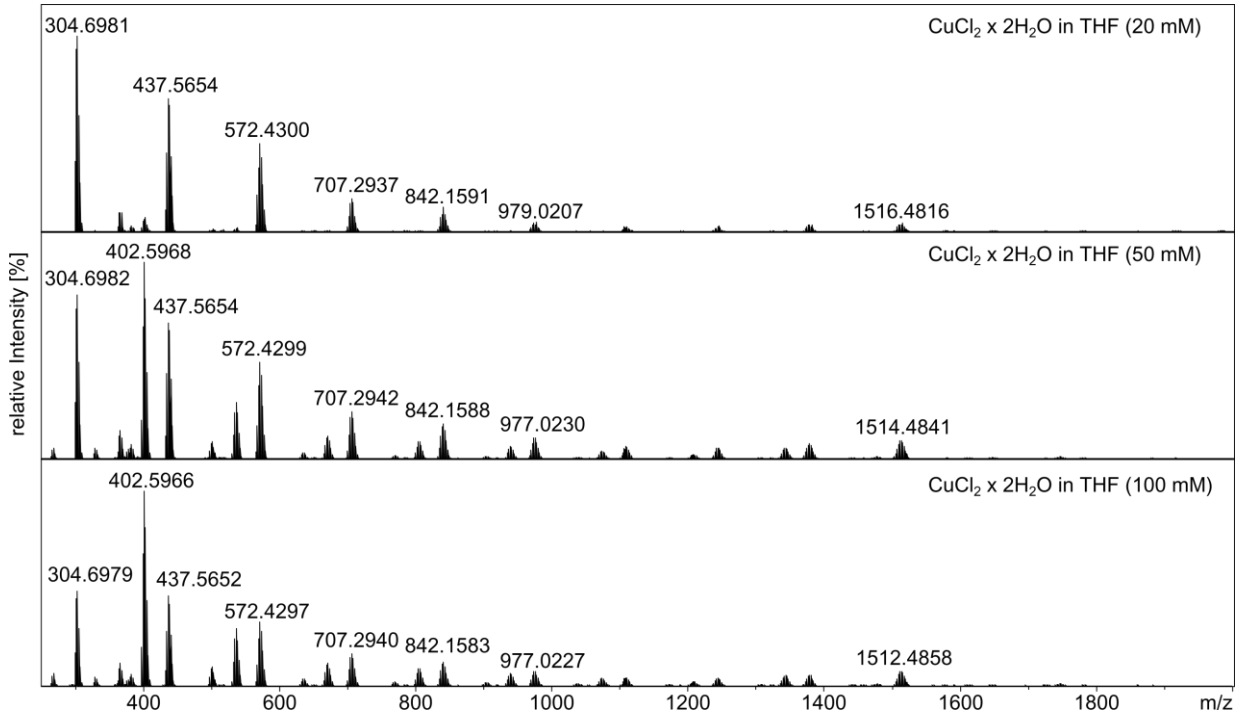

Figure S18: Mass spectrum of $CuCl_2 \cdot 2H_2O$ in THF (negative ion mode), the species identified are listed below.

Table S24: Observed species and m/z for $CuCl_2 \cdot 2H_2O$ in THF (negative ion mode).

Species	**m/z**	**m/z calcd.**
$[Cu_2Cl_5]^-$	304.6981	304.6989
$[Cu_3Cl_7]^-$	437.5654	437.5662
$[Cu_4Cl_9]^-$	572.4300	572.4310
$[Cu_5Cl_{11}]^-$	707.2937	707.2958
$[Cu_6Cl_{13}]^-$	842.1588	842.1606
$[Cu_7Cl_{15}]^-$	977.0207	977.0254

DMF

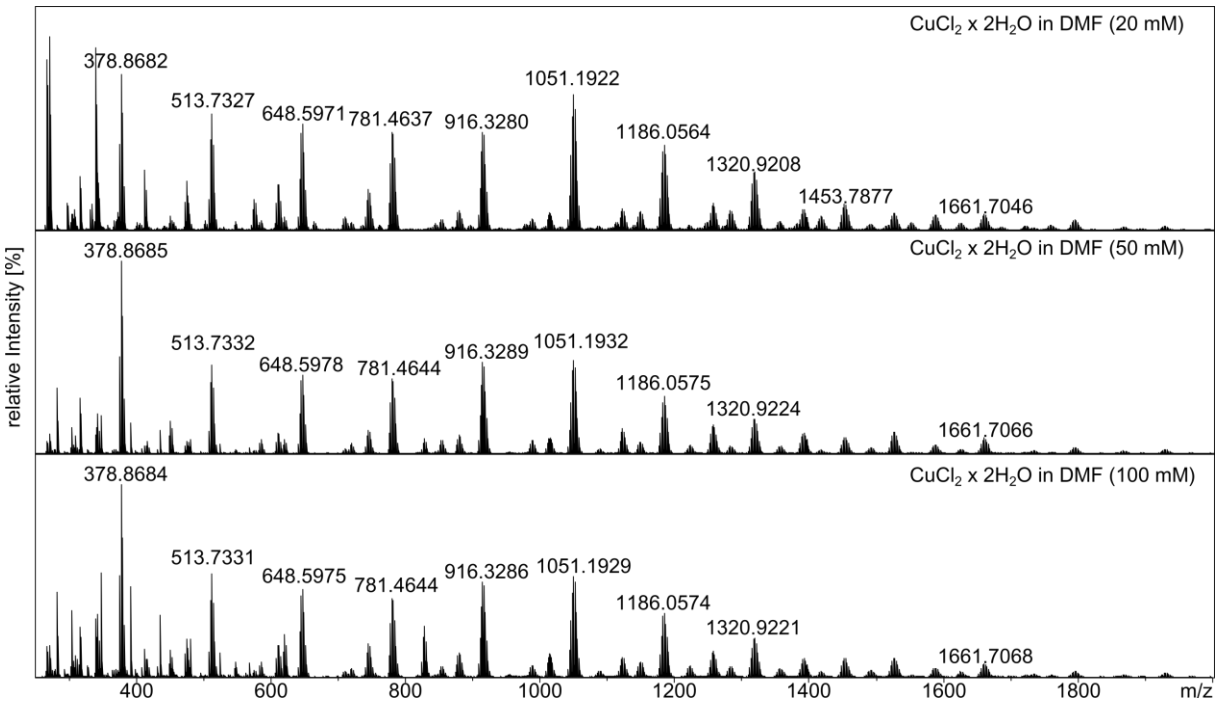

Figure S19: Mass spectrum of $CuCl_2 \cdot 2H_2O$ in DMF (positive ion mode).

Table S25: Observed species and m/z for $CuCl_2 \cdot 2H_2O$ in DMF (positive ion mode).

Species	**m/z**	**m/z calcd.**
$[Cu_2Cl_3(C_3H_7NO)_2]^+$	378.8682	378.8694
$[Cu_3Cl_5(C_3H_7NO)_2]^+$	513.7327	513.7332
$[Cu_4Cl_7(C_3H_7NO)_2]^+$	648.5971	648.5980
$[Cu_5Cl_9(C_3H_7NO)_2]^+$	781.4637	781.4664
$[Cu_6Cl_{11}(C_3H_7NO)_2]^+$	916.3280	916.3307
$[Cu_7Cl_{13}(C_3H_7NO)_2]^+$	1051.1922	1051.1956
$[Cu_8Cl_{15}(C_3H_7NO)_2]^+$	1186.0564	1186.0597

DMSO

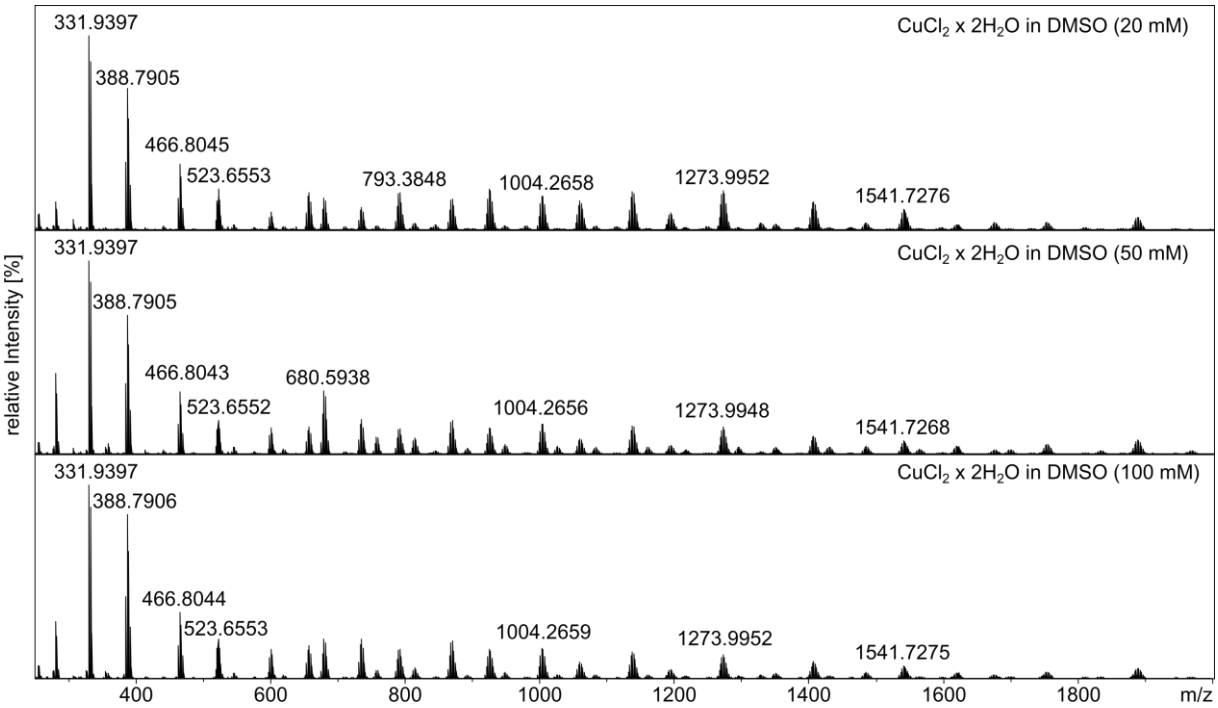

Figure S20: Mass spectrum of $CuCl_2 \cdot 2H_2O$ in DMSO (positive ion mode). Different adducts in the general form of $Cu_nCl_{(2n-1)}(C_2H_6SO)_2$ and $Cu_nCl_{(2n-1)}(C_2H_6SO)_3$ were observed.

Table S26: Observed species and m/z for $CuCl_2 \cdot 2H_2O$ in DMSO (positive ion mode).

Species	**m/z**	**m/z calcd.**
$[Cu_2Cl_3(C_2H_6SO)_2]^+$	388.7905	388.7915
$[Cu_2Cl_3(C_2H_6SO)_3]^+$	466.8045	466.8045
$[Cu_3Cl_5(C_2H_6SO)_2]^+$	523.6553	523.6554
$[Cu_3Cl_5(C_2H_6SO)_3]^+$	601.6690	601.6693
$[Cu_4Cl_7(C_2H_6SO)_2]^+$	658.5200	658.5202
$[Cu_4Cl_7(C_2H_6SO)_3]^+$	736.5338	736.5341
$[Cu_5Cl_9(C_2H_6SO)_2]^+$	793.3848	793.3850
$[Cu_5Cl_9(C_2H_6SO)_3]^+$	871.3984	871.3989
$[Cu_6Cl_{11}(C_2H_6SO)_2]^+$	926.2520	926.2523
$[Cu_6Cl_{11}(C_2H_6SO)_3]^+$	1006.2633	1006.2636
$[Cu_7Cl_{13}(C_2H_6SO)_2]^+$	1061.1165	1061.1171
$[Cu_7Cl_{13}(C_2H_6SO)_3]^+$	1139.1306	1139.1310
$[Cu_8Cl_{15}(C_2H_6SO)_3]^+$	1273.9952	1273.9958

4.2 $CuCl_2 \cdot 2H_2O$ + KO^{t}Bu in selected solvents

Methanol

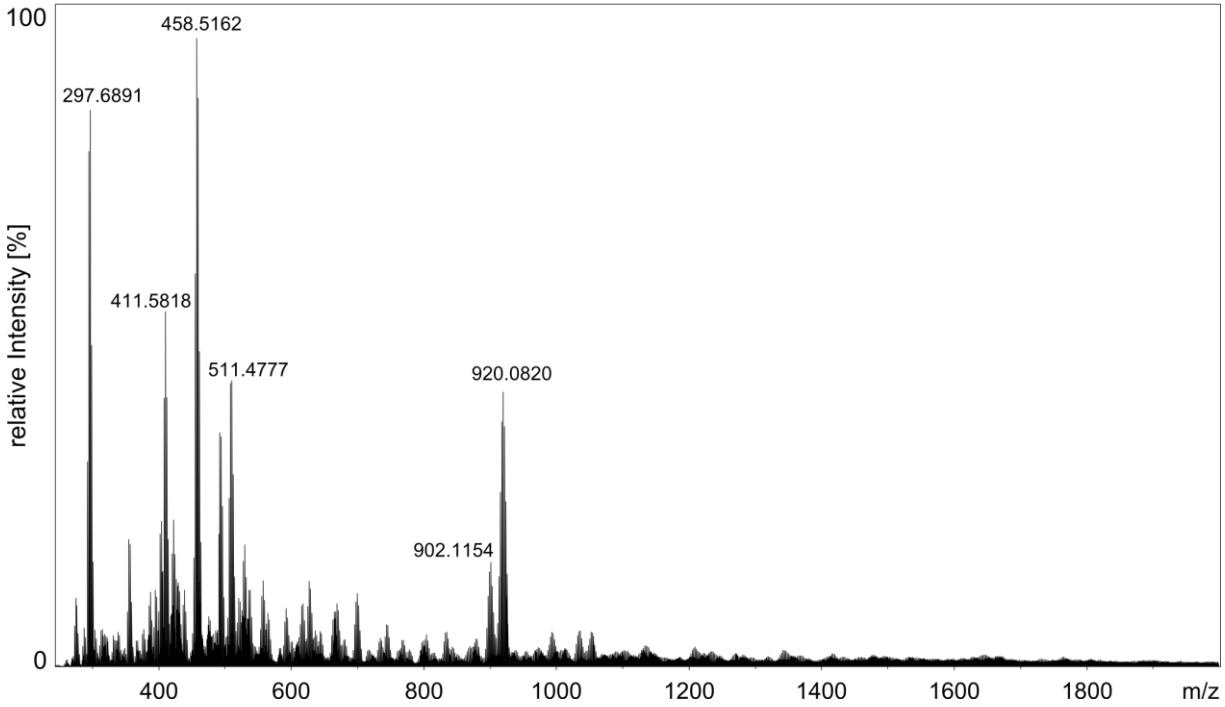

Figure S21: Mass spectrum of $CuCl_2 \cdot 2H_2O$ + KO^{t}Bu (2 eq.) in methanol (50 mM, positive ion mode). The oxidation states of the copper ions are mixed-valent.

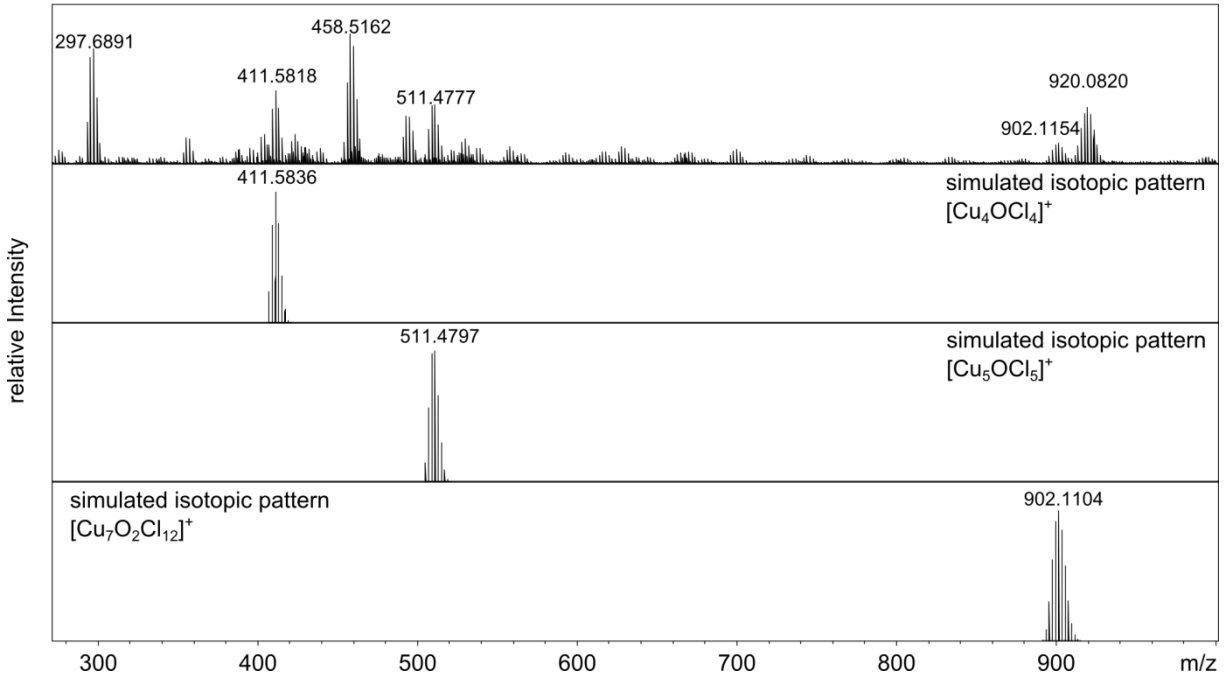

Figure S21-2: Mass spectrum of $CuCl_2 \cdot 2H_2O$ + KO^{t}Bu (2 eq.) in methanol (50 mM, positive ion mode) vs. the simulated isotopic patterns of the observed species

Table S27: Observed species and m/z for $CuCl_2 \cdot 2H_2O$ + KO^{t}Bu (2 eq.) in methanol (50 mM, positive ion mode).

Species	**m/z**	**m/z calcd.**
$[Cu_4OCl_4]^+$	411.5818	411.5836
$[Cu_5OCl_5]^+$	511.4777	511.4797
$[Cu_7O_2Cl_{12}]^+$	902.1154	902.1104

Acetone

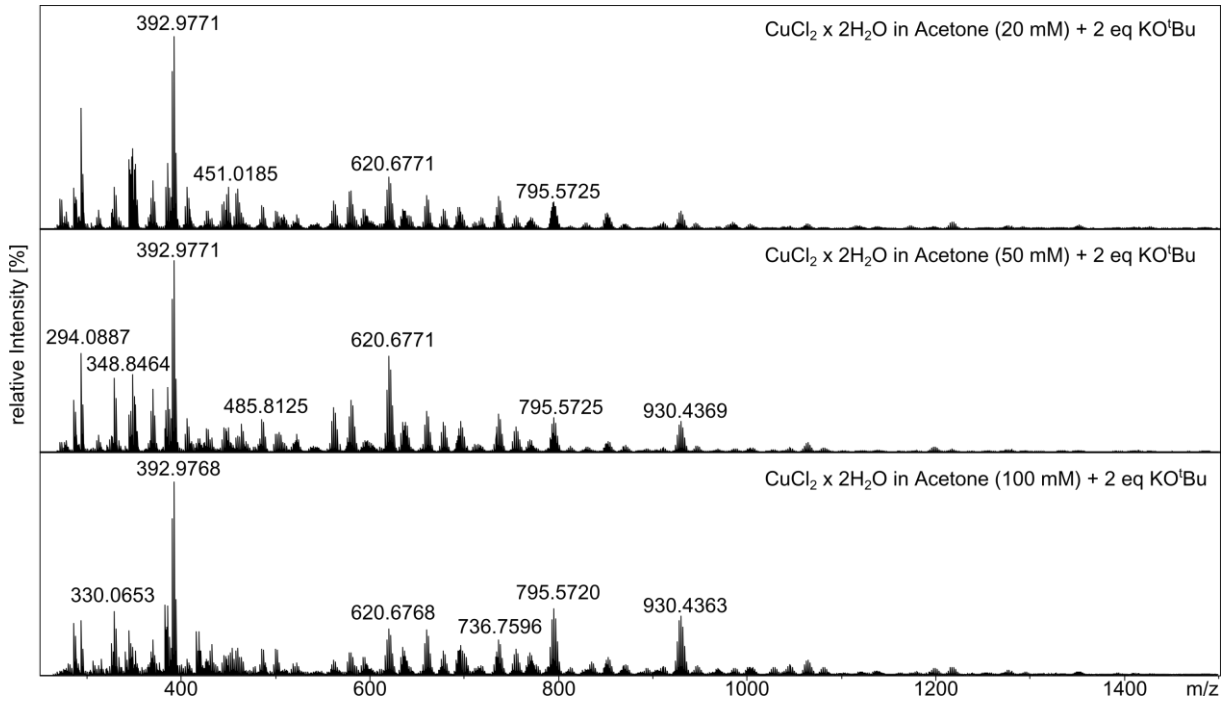

Figure S22: Mass spectrum of $CuCl_2 \cdot 2H_2O$ + KO^{t}Bu in acetone (positive ion mode).

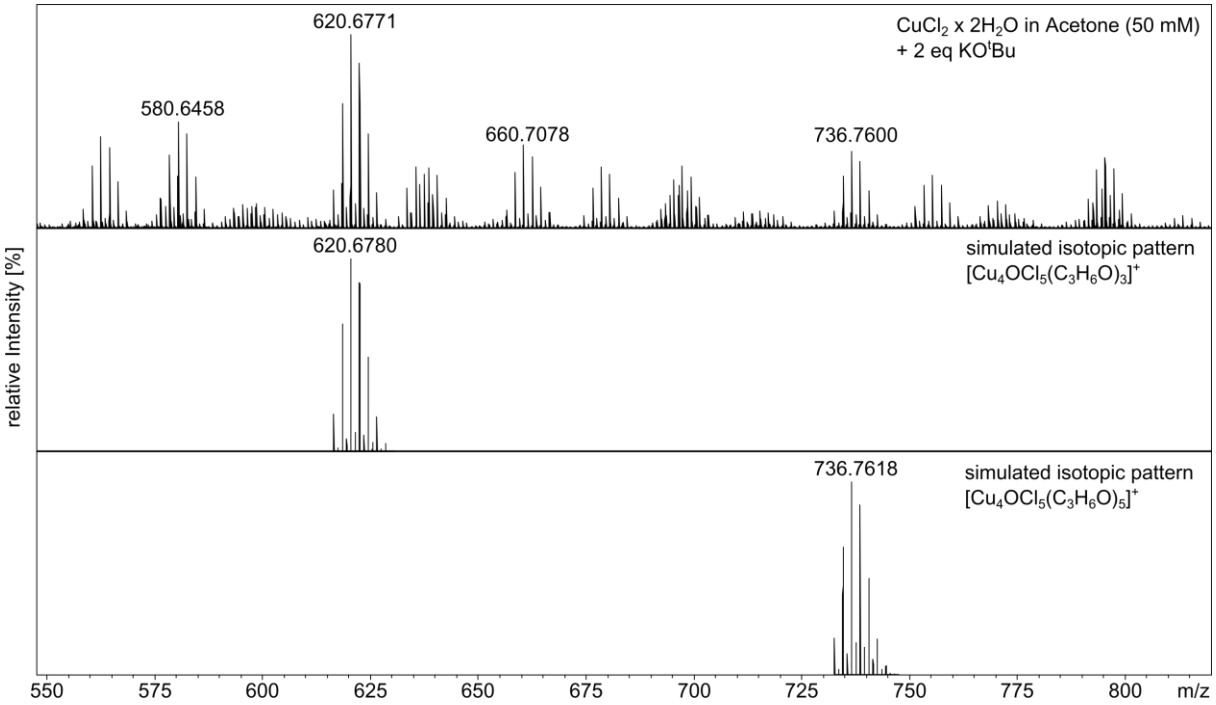

Figure S22-2: Mass spectrum of $CuCl_2 \cdot 2H_2O$ + KO^{t}Bu in acetone (positive ion mode) vs. the simulated isotopic patterns of the observed species

Table S28: Observed species and m/z for $CuCl_2 \cdot 2H_2O$ + KO^{t}Bu in acetone (positive ion mode).

Species	**m/z**	**m/z calcd.**
$[Cu_4OCl_5(C_3H_6O)_2]^+$	562.6350	562.6361
$[Cu_4OCl_5(C_3H_6O)_3]^+$	620.6771	620.6780
$[Cu_4OCl_5(C_3H_6O)_4]^+$	678.7183	678.7199
$[Cu_4OCl_5(C_3H_6O)_5]^+$	736.7603	736.7618

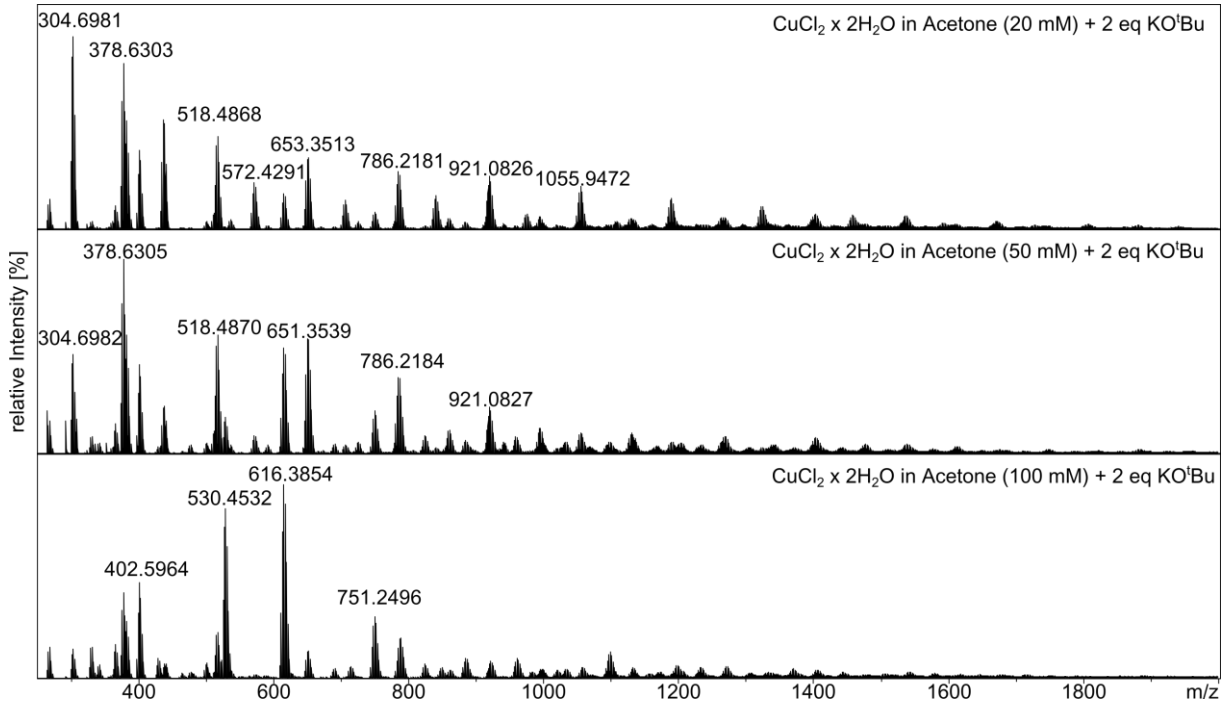

Figure S23: Mass spectrum of $CuCl_2 \cdot 2H_2O$ + KO^{t}Bu in acetone (positive ion mode).

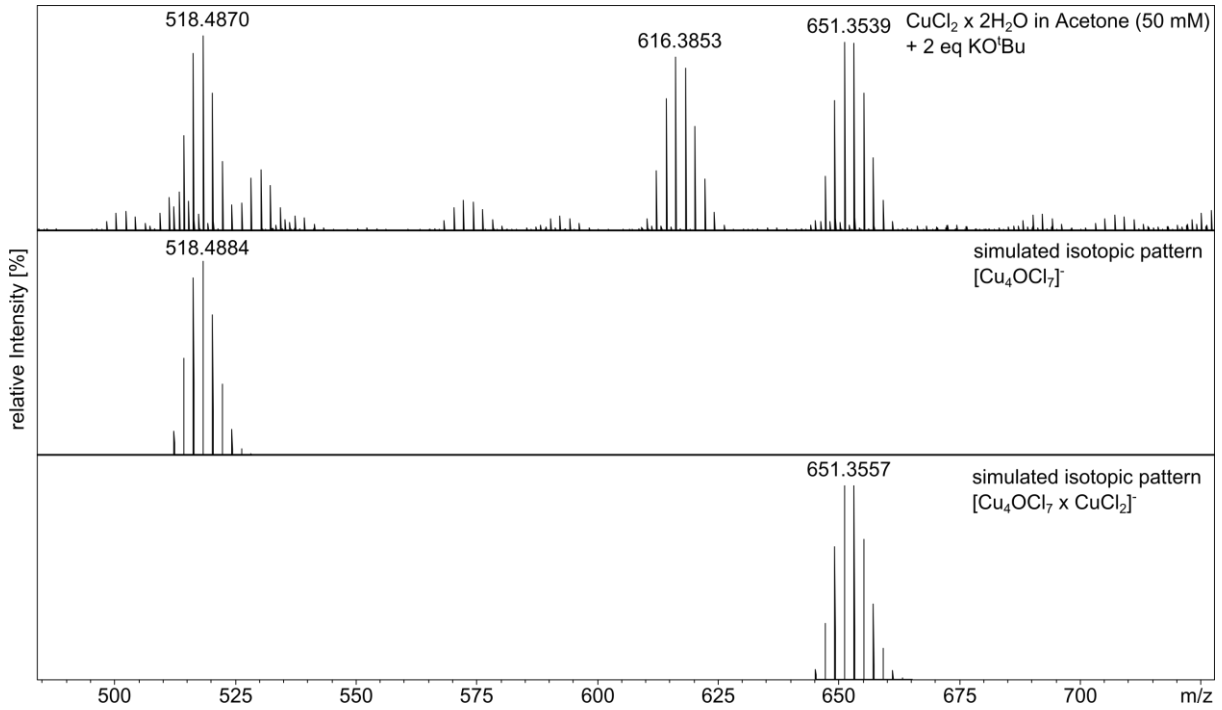

Figure S23-2: Mass spectrum of $CuCl_2 \cdot 2H_2O$ + KO^{t}Bu in acetone (positive ion mode) vs. the simulated isotopic patterns of the observed species

Table S29: Observed species and m/z for $CuCl_2 \cdot 2H_2O$ + KO^{t}Bu in acetone (positive ion mode).

Species	**m/z**	**m/z calcd.**
$[Cu_4OCl_7]^-$	518.4884	518.4868
$[Cu_4OCl_7(CuCl_2)]^-$	653.3532	653.3513
$[Cu_4OCl_7(CuCl_2)_2]^-$	786.2205	786.2181
$[Cu_4OCl_7(CuCl_2)_3]^-$	921.0853	921.0826

Acetonitrile

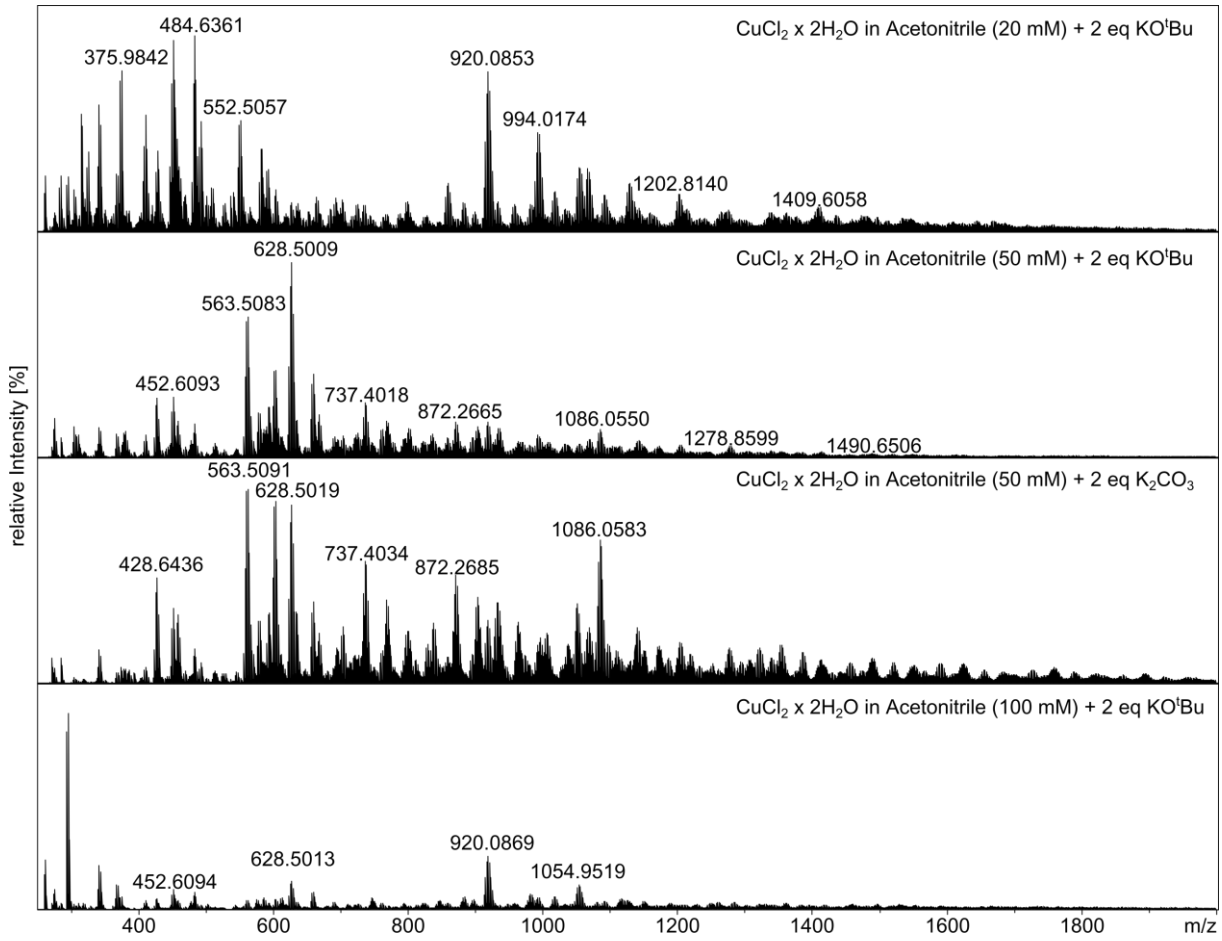

Figure S24: Mass spectrum of $CuCl_2 \cdot 2H_2O$ + KOtBu/K_2CO_3 in acetonitrile (positive ion mode). The oxidation states of the copper ions are mixed-valent.

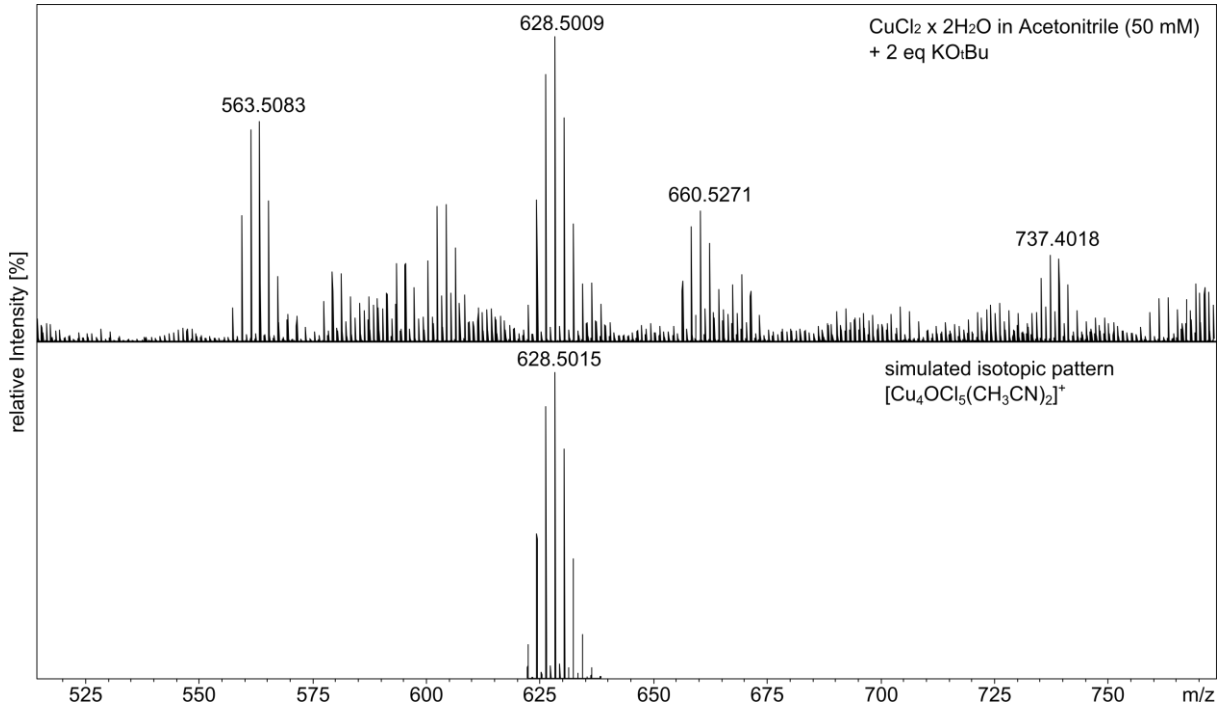

Figure S24-2: Mass spectrum of $CuCl_2 \cdot 2H_2O$ + KO^{t}Bu in acetone (positive ion mode) vs. the simulated isotopic patterns of the observed species

Table S30: Observed species and m/z for $CuCl_2 \cdot 2H_2O$ + KO^{t}Bu in acetonitrile (positive ion mode).

Species	**m/z**	**m/z calcd.**
$[Cu_4OCl_4(CH_3CN)]^+$	452.6099	452.6101
$[Cu_4OCl_4(CH_3CN)_2]^+$	493.6363	493.6367
$[Cu_5OCl_5(CH_3CN)]^+$	552.5057	552.5063
$[Cu_4OCl_5(CH_3CN)_2]^+$	628.5009	628.5015

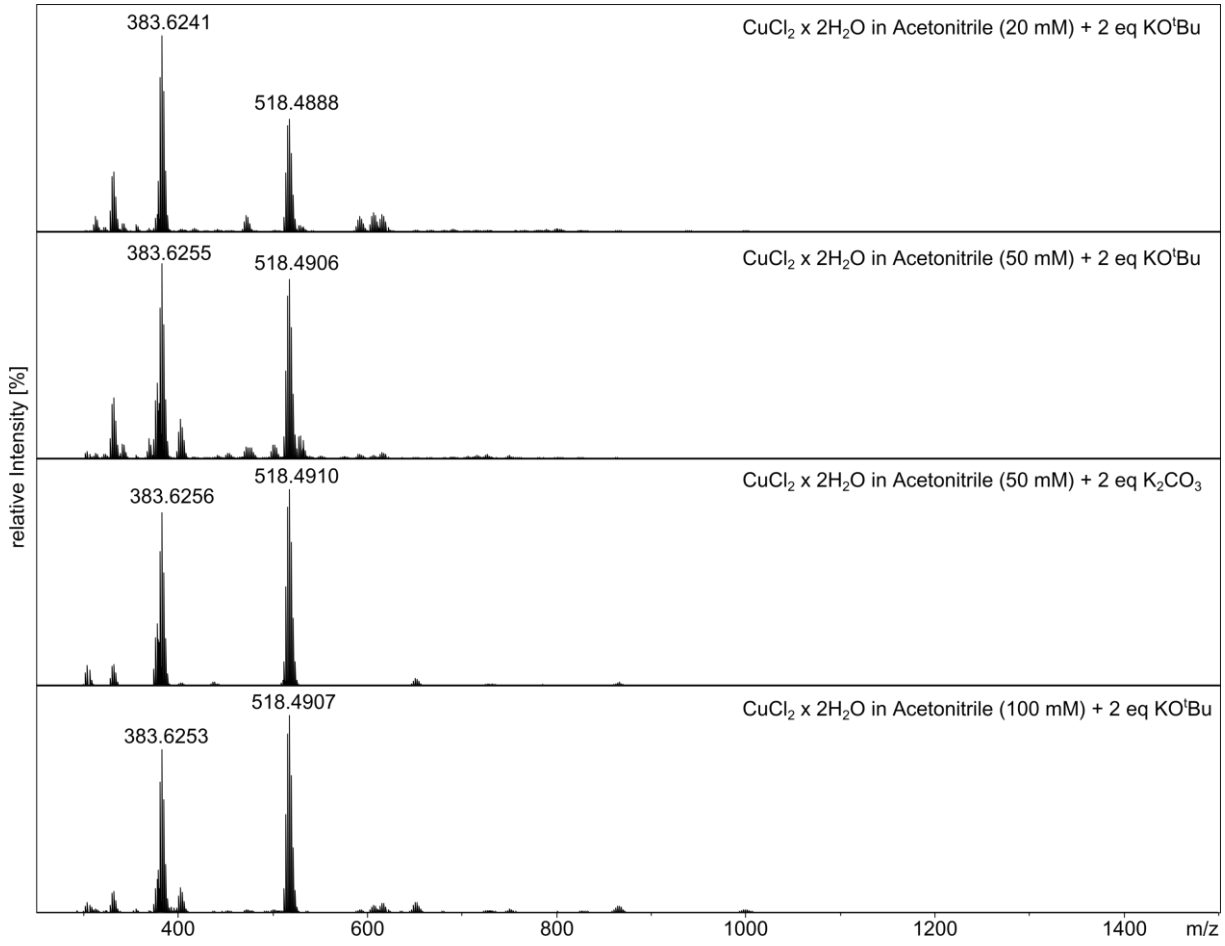

Figure S25: Mass spectrum of $CuCl_2 \cdot 2H_2O$ + KO^{t}Bu/K_2CO_3 in acetonitrile (negative ion mode).

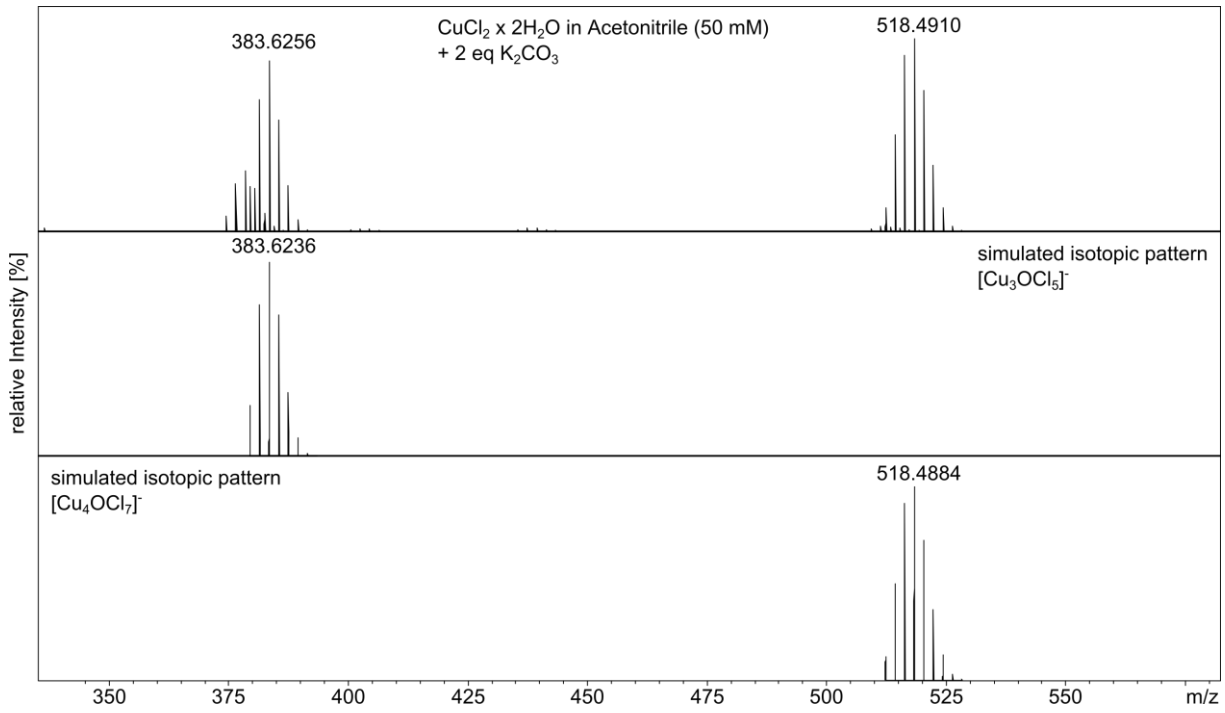

Figure S25-2: Mass spectrum of $CuCl_2 \cdot 2H_2O$ + KO^{t}Bu in acetone (negative ion mode) vs. the simulated isotopic patterns of the observed species

Table S31: Observed species and m/z for $CuCl_2 \cdot 2H_2O$ + K_2CO_3 in acetonitrile (negative ion mode).

Species	**m/z**	**m/z calcd.**
$[Cu_3OCl_5]^-$	383.6256	383.6236
$[Cu_4OCl_7]^-$	518.4910	518.4884

THF

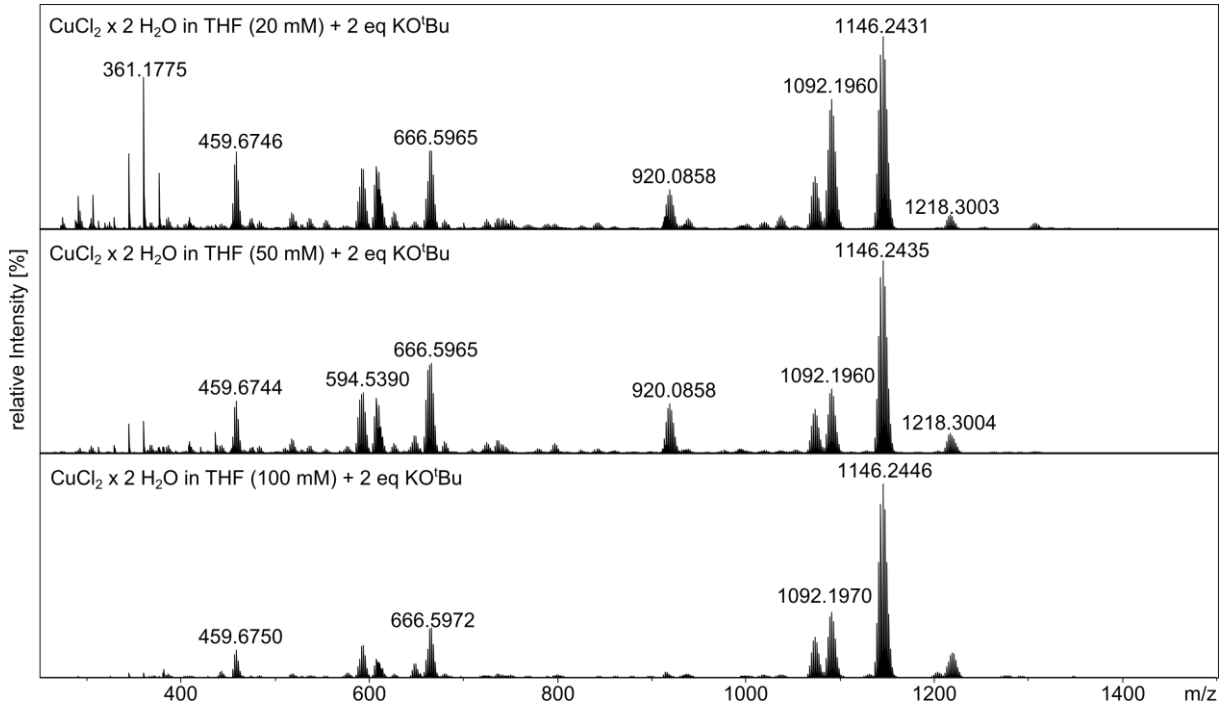

Figure S26: Mass spectrum of $CuCl_2 \cdot 2H_2O$ + KOtBu in THF (positive ion mode).

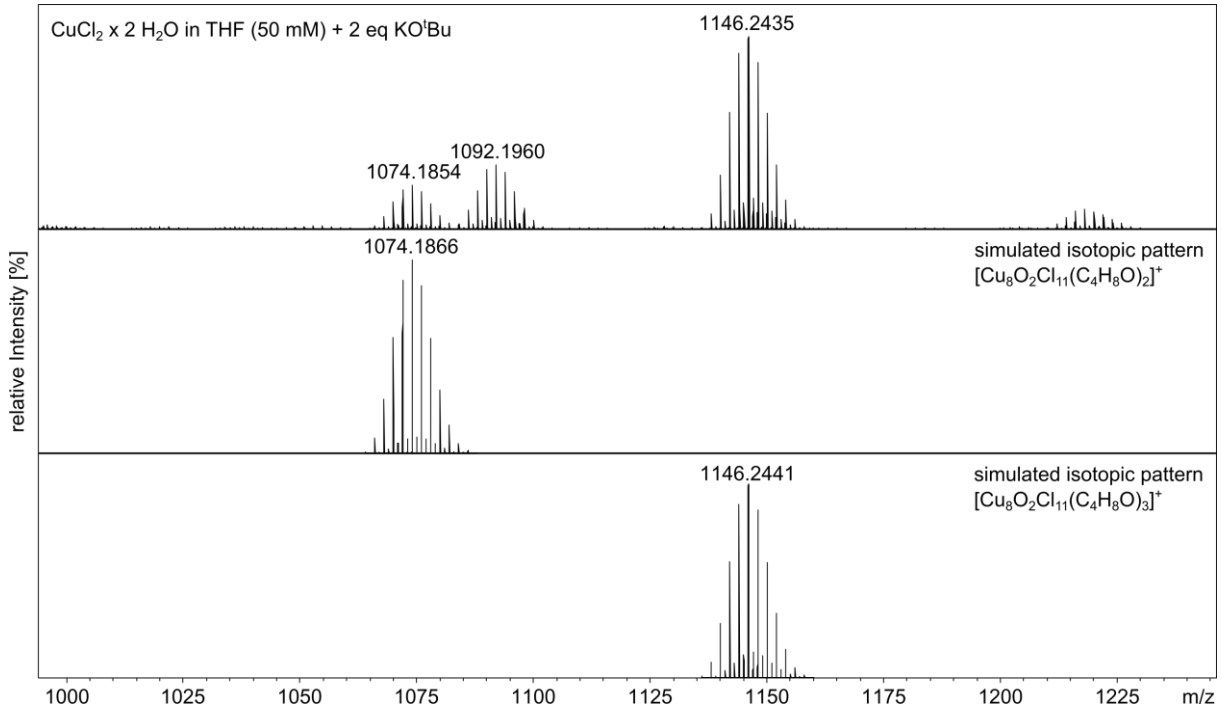

Figure S26-2: Mass spectrum of $CuCl_2 \cdot 2H_2O$ + KO^{t}Bu in THF (positive ion mode) vs. the simulated isotopic patterns of the observed species

Table S32: Observed species and m/z for $CuCl_2 \cdot 2H_2O$ + KO^{t}Bu in THF (positive ion mode).

Species	**m/z**	**m/z calcd.**
$[Cu_8O_2Cl_{11}(C_4H_8O)_2]^+$	1074.1854	1074.1866
$[Cu_8O_2Cl_{11}(C_4H_8O)_2(H_2O)]^+$	1092.1960	1092.1971
$[Cu_8O_2Cl_{11}(C_4H_8O)_3]^+$	1146.2435	1146.2441
$[Cu_8O_2Cl_{11}(C_4H_8O)_4]^+$	1218.3004	1218.3017

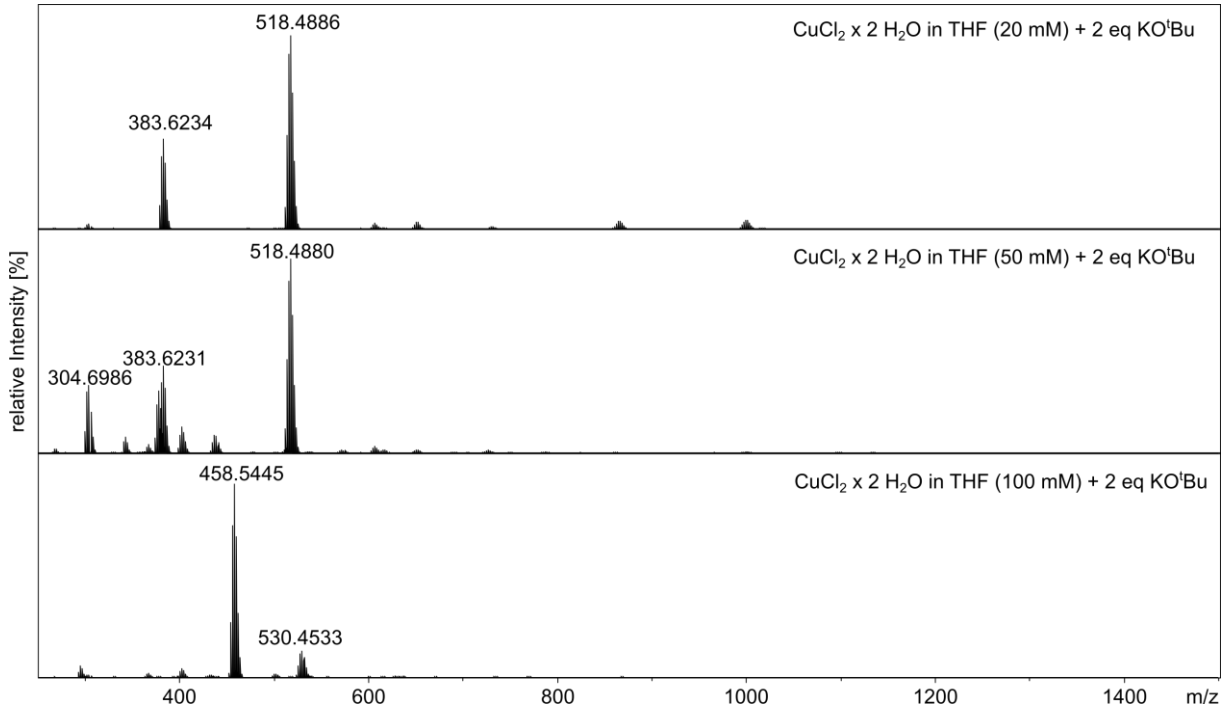

Figure S27: Mass spectrum of $CuCl_2 \cdot 2H_2O$ + KOtBu in THF (negative ion mode).

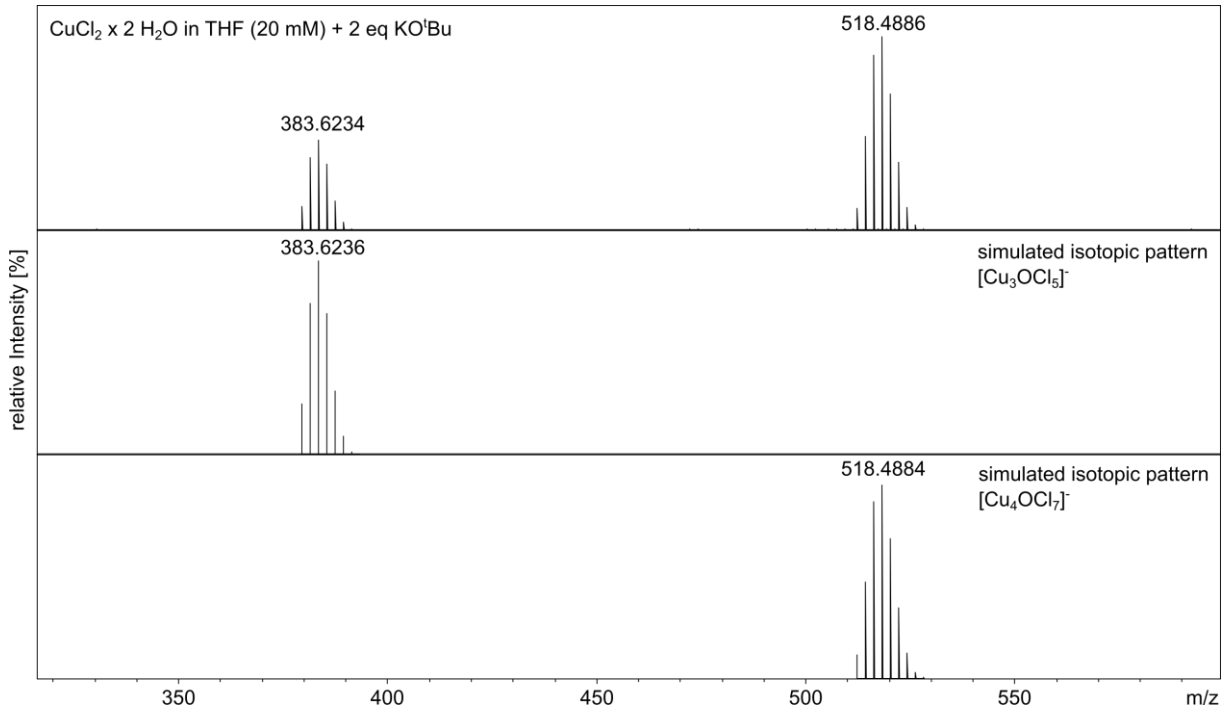

Figure S27-2: Mass spectrum of $CuCl_2 \cdot 2H_2O$ + KO*t*Bu in THF (negative ion mode) vs. the simulated isotopic patterns of the observed species

Table S33: Observed species and m/z for $CuCl_2 \cdot 2H_2O$ + KO*t*Bu in THF (negative ion mode).

Species	**m/z**	**m/z calcd.**
$[Cu_3OCl_5]^-$	383.6234	383.6236
$[Cu_4OCl_7]^-$	518.4886	518.4884

DMF

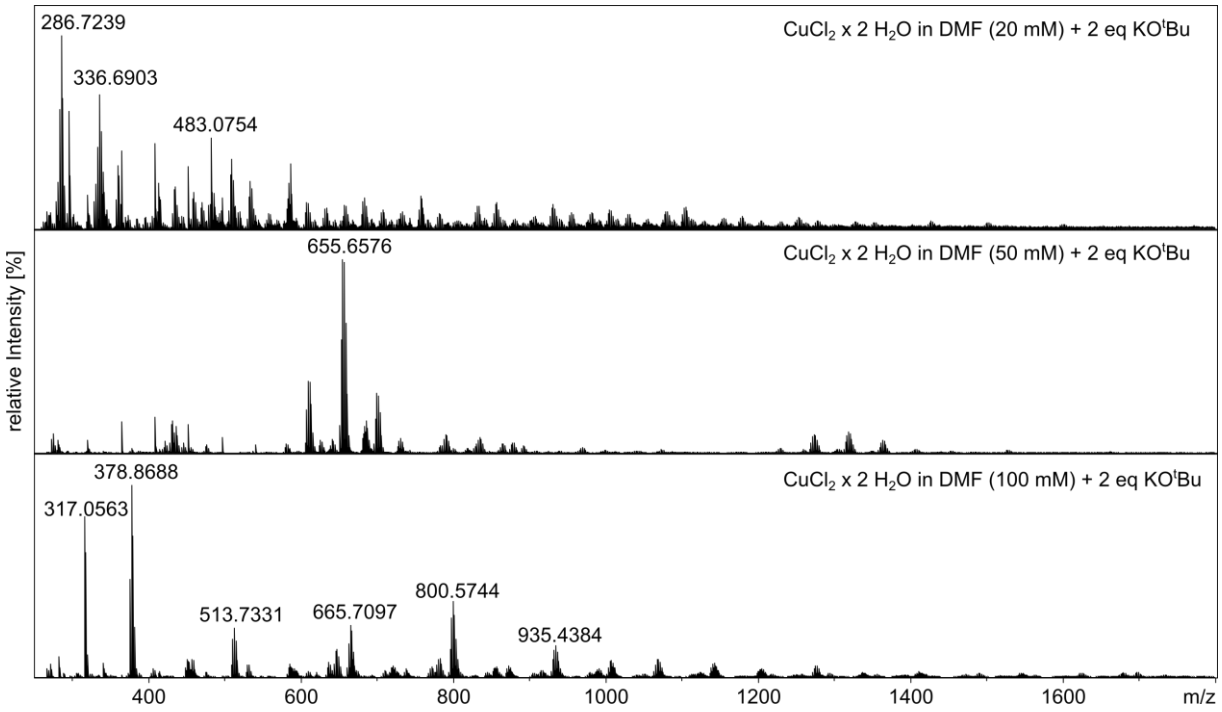

Figure S28: Mass spectrum of $CuCl_2 \cdot 2H_2O$ + KOtBu in DMF (positive ion mode).

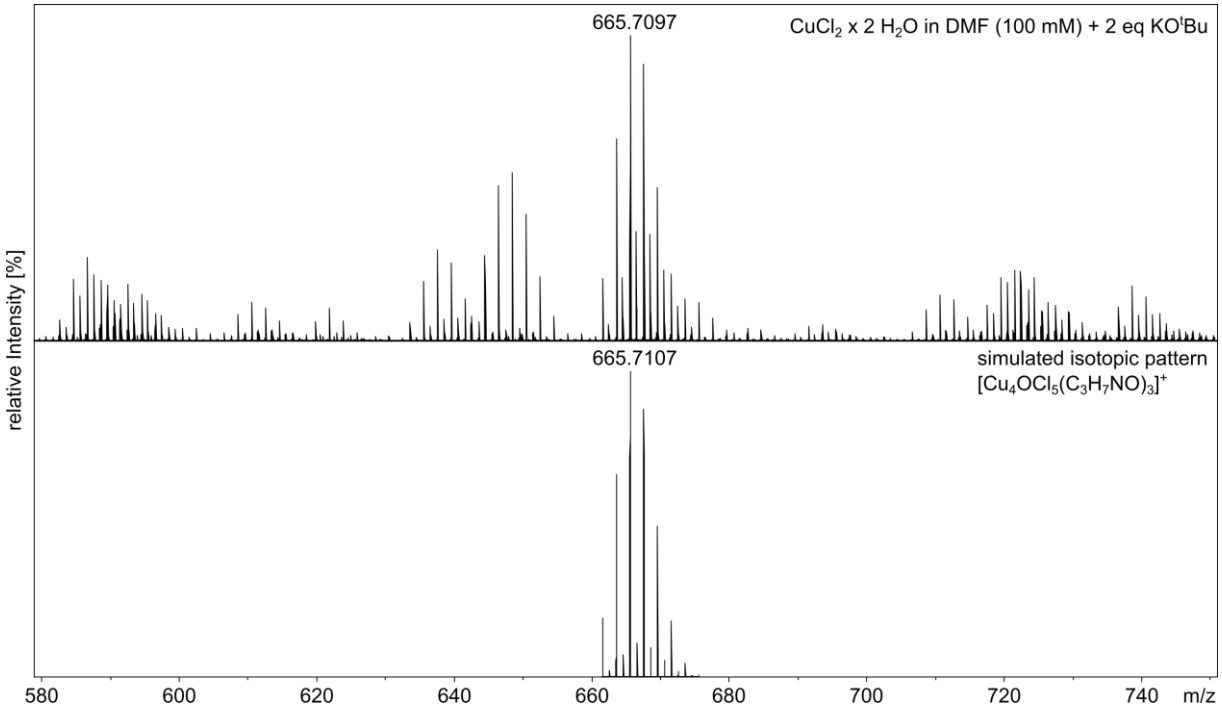

Figure S28-2: Mass spectrum of $CuCl_2 \cdot 2H_2O$ + KO*t*Bu in DMF (positive ion mode) vs. the simulated isotopic patterns of the observed species

Table S34: Observed species and m/z for $CuCl_2 \cdot 2H_2O$ + KO^{t}Bu in DMF (positive ion mode).

Species	**m/z**	**m/z calcd.**
$[Cu_4OCl_5(C_3H_7NO)_3]^+$	665.7097	665.7107

DMSO

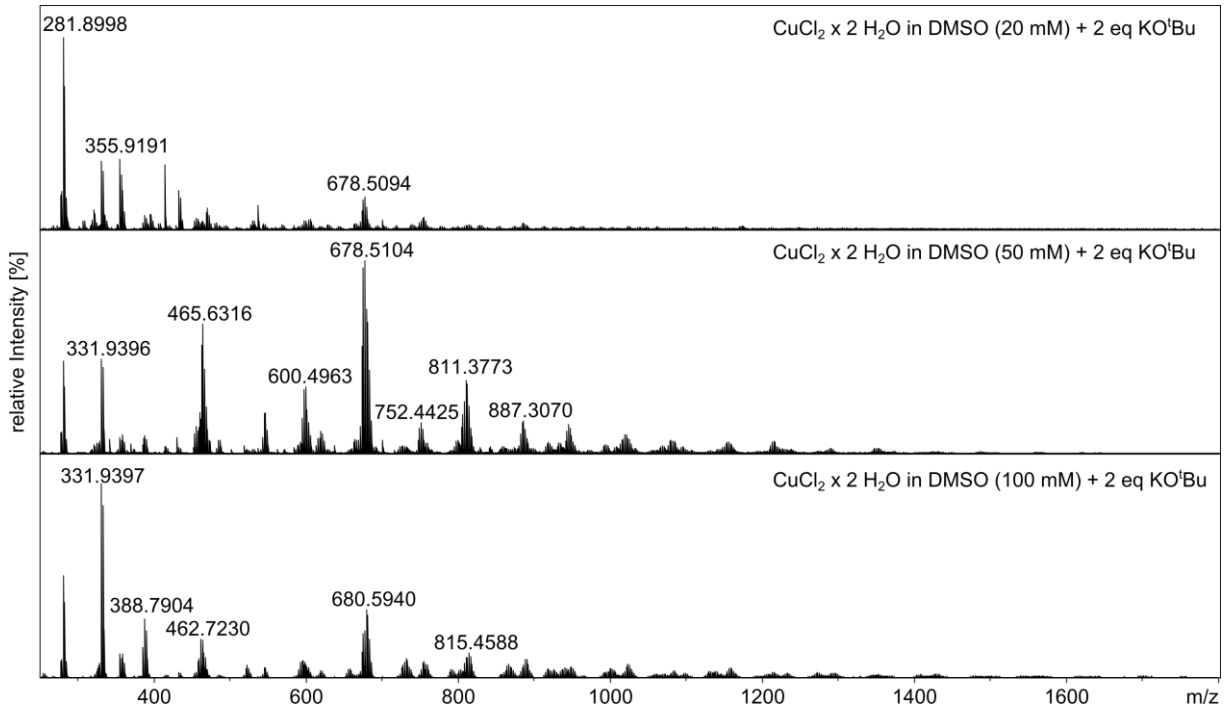

Figure S29: Mass spectrum of $CuCl_2 \cdot 2H_2O$ + KO^{t}Bu in DMSO (positive ion mode).

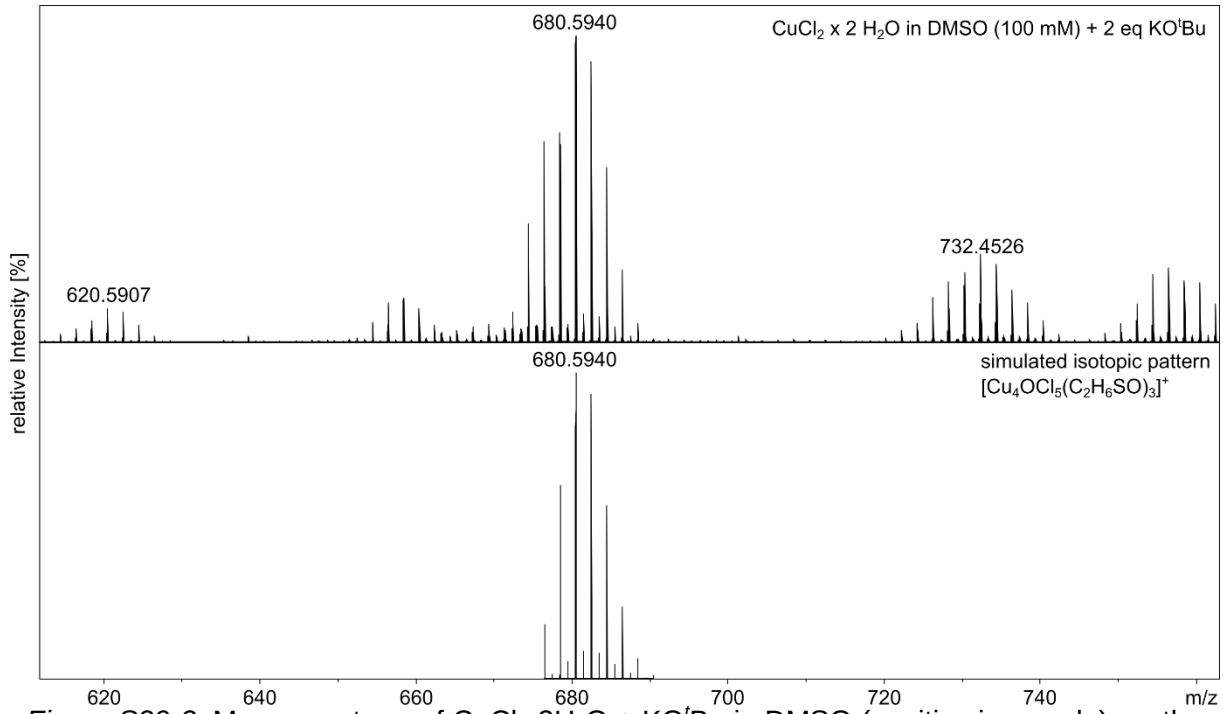

Figure S29-2: Mass spectrum of $CuCl_2 \cdot 2H_2O$ + KO^{t}Bu in DMSO (positive ion mode) vs. the simulated isotopic patterns of the observed species

Table S35: Observed species and m/z for $CuCl_2 \cdot 2H_2O$ + KO^{t}Bu in DMSO (positive ion mode).

Species	**m/z**	**m/z calcd.**
$[Cu_4OCl_5(DMSO)_3]^+$	680.5940	680.5940

4. Infrared Spectroscopy and Elemental Analyses

4.1 Compound 3: $[Cu_3Cl_6(acetonitrile)_2]\cdot CuCl_2$

Elemental analysis:
C: 8.8% H: 1.2% N: 4.6% (Experimental)
C: 7.8% H: 1.0% N: 4.5% (Theoretical)

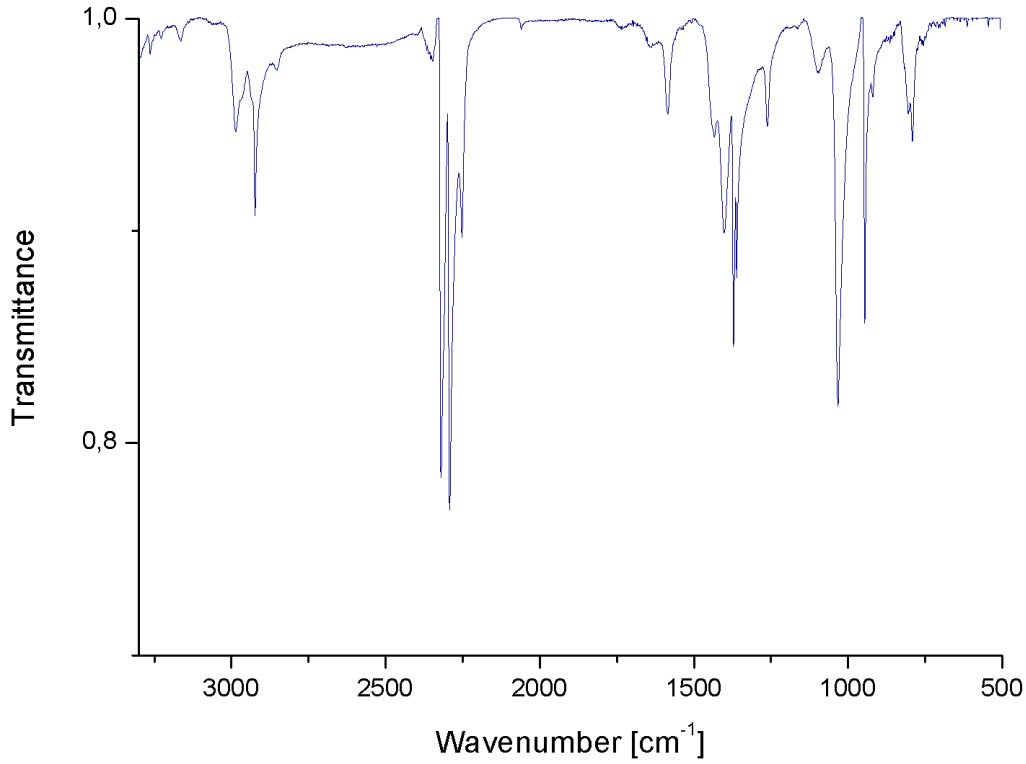

Figure S30: Infrared spectrum of **3**.

Table S36: Infrared data of **3**.

2982-2921 cm^{-1}	$\nu(CH_2)$
2316-2285 cm^{-1}	$\nu(CN)$
1399-1368 cm^{-1}	$\delta(CH)$

4.2 Compound 4: $[Cu(DMSO)_2Cl_2]$

Elemental analysis:
C: 16.5% H: 4.1% N: 0.0% (Experimental)
C: 16.5% H: 4.2% N: 0.0% (Theoretical)

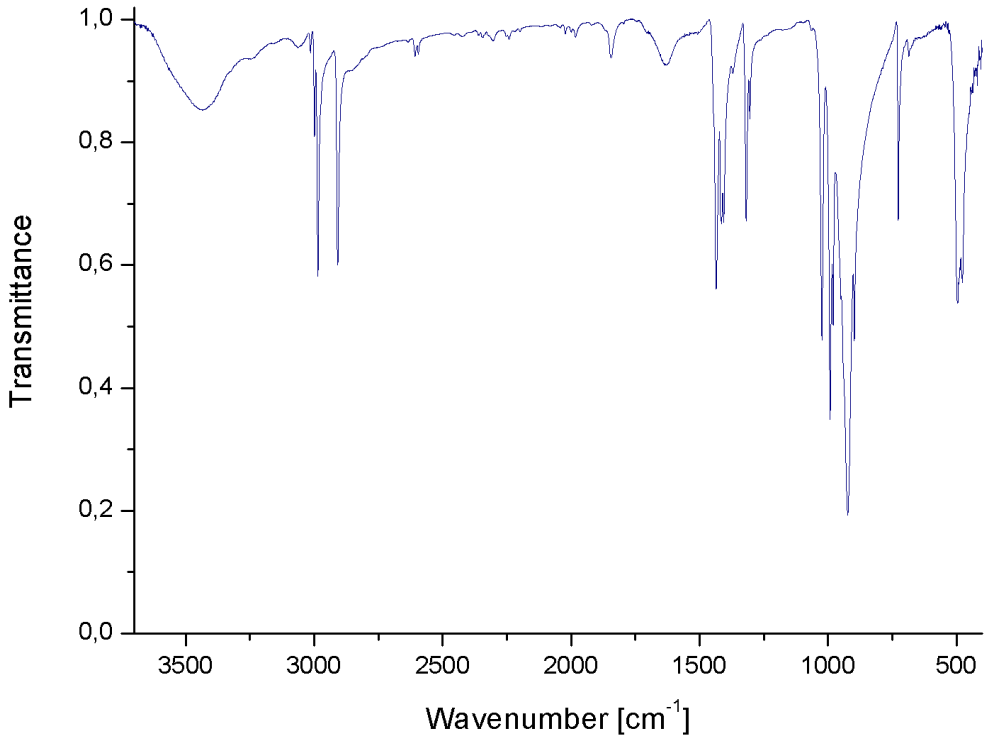

Figure S31: Infrared spectrum of **4**.

Table S37: Infrared data of **4**.

2985-2908 cm^{-1}	$\nu(CH_2)$
1435 cm^{-1}	$\delta(CH_2)$
991 cm^{-1}	$\nu(S=O)$

4.3 Compound 6: $[Cu_4OCl_6(MeOH)_4]$

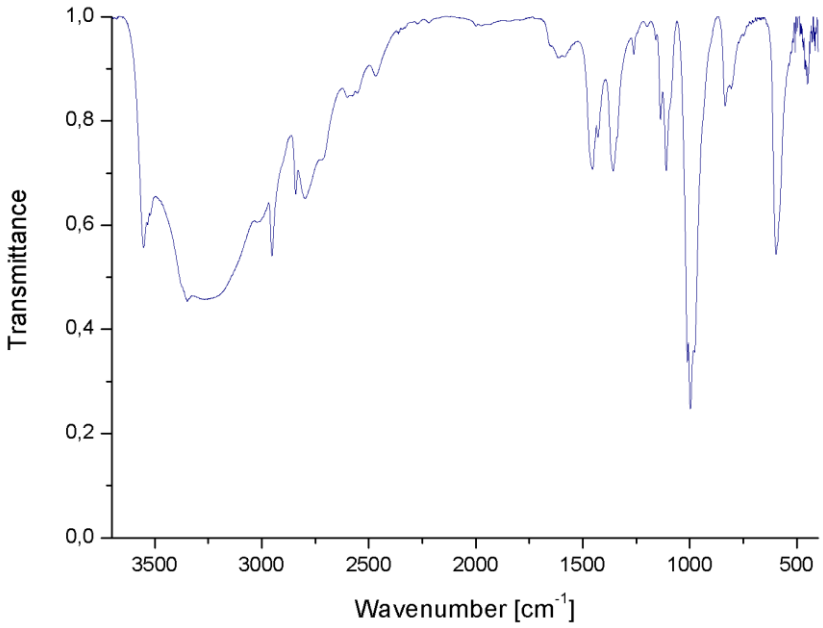

Figure S32: Infrared spectrum of **7**.

Table S38: Infrared data of **7**.

3549-2951 cm^{-1}	v(OH)
2803 cm^{-1}	v(CH_2)
1455 cm^{-1}	δ(CH)
1109 cm^{-1}	v(C-O)
597 cm^{-1}	v(Cu_4O)

4.4 Comparison of $[Cu_4OCl_6(MeOH)_4]$ and 7

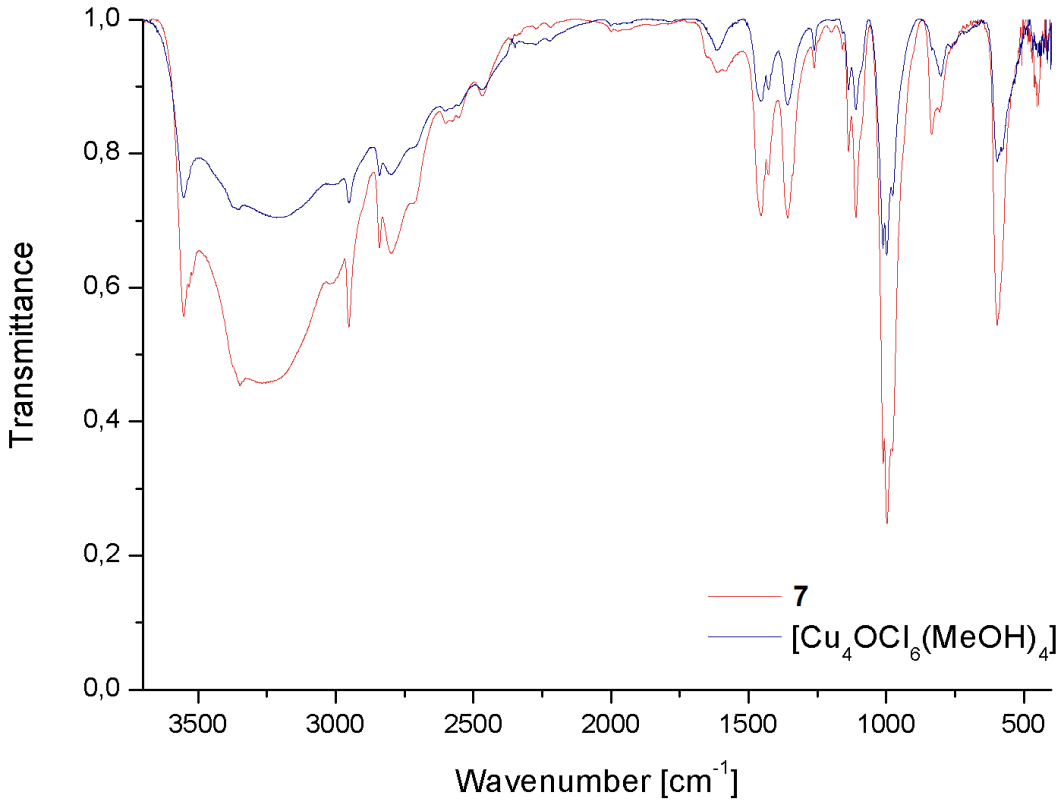

Figure S33: Infrared spectra of **7** and $[Cu_4OCl_6(MeOH)_4]$.